conditions such as essential tremor, progressive supranuclear palsy, and multiple system atrophy.[25,26] In this regard, some patients with 2 allele *parkin* mutations without Lewy bodies were reported to have normal ^{123}I-MIBG uptake.[27,28] Another study demonstrated markedly low heart to mediastinum ratios in patients with classic PD with Lewy bodies and in incidental Lewy body disease, suggesting that Lewy body pathology itself may be responsible for low ^{123}I-MIBG uptake.[30] Although a single case with a homozygous *PINK1* mutation was reported to have a very mild decrease in ^{123}I-MIBG uptake,[31] our data showed that 2 patients with homozygous *PINK1* mutations (patient B with disease duration of 10 years and patient C with disease duration of 2 years) had normal myocardial ^{123}I-MIBG uptake. In contrast, 3 patients with single heterozygous *PINK1* mutations (patients E, H, and J) had low myocardial ^{123}I-MIBG uptake. These findings suggest that patients with a single heterozygous mutation are more likely to have cardiac sympathetic denervation than those with homozygous *PINK1* mutations, which accounts for the low ^{123}I-MIBG uptake. One can further speculate that patients with heterozygous *PINK1* mutations may have Lewy body pathology, whereas those with homozygous *PINK1* mutations have no Lewy body pathology, similar to patients with *parkin* mutations,[10,32] though no pathologic study of patients with 2 allele *PINK1* mutations has been reported to date. Additional studies of cardiac scintigraphy in a larger number of *PINK1*-positive patients with PD are required to clarify these points.

In summary, we assume that homozygous *PINK1* mutations may manifest in an early-onset autosomal recessive form of PD. We can also speculate that single heterozygous mutations may be 1 of the risk factors in developing the sporadic or autosomal dominant form of PD. Additional studies are necessary to clarify the etiopathogenic roles of 1 allele *PINK1* mutation in developing various forms of PD.

Accepted for Publication: December 19, 2007.
Author Affiliations: Department of Neurology (Drs Kumazawa, Tomiyama, Li, and Hattori and Ms Imamichi), and Research Institute for Diseases of Old Age (Drs Funayama and Mizuno and Ms Yoshino), Juntendo University School of Medicine, Tokyo, Japan; Department of Neurology, Tokyo Metropolitan Neurological Hospital, Tokyo, Japan (Dr Yokochi); Department of Neurology, Yamaguchi Grand Medical Center, Yamaguchi, Japan (Dr Fukusako); Department of Neurology, Graduate School of Medicine and Dentistry Okayama University, Okayama, Japan (Dr Takehisa); Department of Neurology, Okayama Kyokuto Hospital, Okayama, Japan (Dr Kashihara); Department of Neurology, Wakayama Medical University, Wakayama, Japan (Dr Kondo); Department of Neurology, Institute of Neurological Sciences and Psychiatry, Hacettepe University School of Medicine, Ankara, Turkey (Dr Elibol); Third University Department of Neurology, G. Papanikolaou Hospital, Thessaloniki, Greece (Dr Bostantjopoulou); Core Research for Evolutional Science and Technology, Japan Science and Technology Corporation, Saitama, Japan (Drs Toda and Hattori); and Department of Neurology, Tokai University School of Medicine, Kanagawa, Japan (Drs Takahashi and Yoshii).
Correspondence: Nobutaka Hattori, MD, PhD, Department of Neurology, Juntendo University School of Medicine, 2-1-1 Hongo, Bunkyo, Tokyo 113-8421, Japan (nhattori@med.juntendo.ac.jp).
Author Contributions: *Study concept and design:* Kumazawa, Li, and Hattori. *Acquisition of data:* Kumazawa, Li, and Hattori. *Analysis and interpretation of data:* Kumazawa, Tomiyama, Li, Imamichi, Funayama, Yoshino, Yokochi, Fukusako, Takehisa, Kashihara, Kondo, Elibol, Bostantjopoulou, Toda, Takahashi, Yoshii, Mizuno, and Hattori. *Drafting of the manuscript:* Kumazawa, Tomiyama, Li, Imamichi, Funayama, Yoshino, Yokochi, Fukusako, Takehisa, Kashihara, Kondo, Elibol, Bostantjopoulou, Toda, Takahashi, Yoshii, Mizuno, and Hattori. *Critical revision of the manuscript for important intellectual content:* Kumazawa and Hattori. *Statistical analysis:* Kumazawa and Hattori. *Obtained funding:* Mizuno and Hattori. *Administrative, technical, and material support:* Kumazawa, Li, Imamichi, Yoshino, Yokochi, Fukusako, Takehisa, Kashihara, Kondo, Elibol, Bostantjopoulou, and Toda. *Study supervision:* Kumazawa, Tomiyama, Funayama, Takahashi, Yoshii, Mizuno, and Hattori.
Financial Disclosure: None reported.
Additional Contributions: We thank the patients and their family members who participated in this study.

REFERENCES

1. Lang AE, Lozano AM. Parkinson's disease: second of two parts. *N Engl J Med*. 1998;339(16):1130-1143.
2. Polymeropoulos MH, Lavedan C, Leroy E, et al. Mutation in the alphasynuclein gene identified in families with Parkinson's disease. *Science*. 1997;276(5321):2045-2047.
3. Leroy E, Boyer R, Auburger G, et al. The ubiquitin pathway in Parkinson's disease. *Nature*. 1998;395(6701):451-452.
4. Harhangi BS, Farrer MJ, Lincoln S, et al. The Ile93Met mutation in the ubiquitin carboxy-terminal-hydrolase-L1 gene is not observed in European cases with familial Parkinson's disease. *Neurosci Lett*. 1999;270(1):1-4.
5. Paisán-Ruiz C, Jain S, Evans EW, et al. Cloning of the gene containing mutations that cause PARK8-linked Parkinson's disease. *Neuron*. 2004;44(4):595-600.
6. Zimprich A, Biskup S, Leitner P, et al. Mutations in LRRK2 cause autosomal dominant parkinsonism with pleomorphic pathology. *Neuron*. 2004;44(4):601-607.
7. Kitada T, Asakawa S, Hattori N, et al. Mutations in the parkin gene cause autosomal recessive juvenile parkinsonism. *Nature*. 1998;392(6676):605-608.
8. Bonifati V, Rizzu P, van Baren MJ, et al. Mutations in the DJ-1 gene associated with autosomal recessive early-onset parkinsonism. *Science*. 2003;299(5604):256-259.
9. Valente EM, Abou-Sleiman PM, Caputo V, et al. Hereditary early-onset Parkinson's disease caused by mutations in PINK1. *Science*. 2004;304(5674):1158-1160.
10. Lücking CB, Durr A, Bonifati V, et al. Association between early-onset Parkinson's disease and mutations in the parkin gene. *N Engl J Med*. 2000;342(21):1560-1567.
11. Hattori N, Mizuno Y. Pathogenetic mechanisms of parkin in Parkinson's disease. *Lancet*. 2004;364(9435):722-724.
12. Groen JL, Kawarai T, Toulina A, et al. Genetic association study of PINK1 coding polymorphisms in Parkinson's disease. *Neurosci Lett*. 2004;372(3):226-229.
13. Hughes AJ, Daniel SE, Kilford L, Lees AJ. Accuracy of clinical diagnosis of idiopathic Parkinson's disease: a clinico-pathological study of 100 cases. *J Neurol Neurosurg Psychiatry*. 1992;55(3):181-184.
14. Hatano Y, Li Y, Sato K, et al. Novel PINK1 mutations in early-onset parkinsonism. *Ann Neurol*. 2004;56(3):424-427.
15. Li Y, Tomiyama H, Sato K, et al. Clinicogenetic study of PINK1 mutations in autosomal recessive early-onset parkinsonism. *Neurology*. 2005;64(11):1955-1957.

16. Zhang YH, Tang BS, Guo JF, et al. Mutation analysis of PINK1 gene in Chinese patients with autosomal recessive early-onset parkinsonism type 6. *Zhonghua Yi Xue Za Zhi*. 2005;85(22):1538-1541.
17. Hatano Y, Sato K, Elibol B, et al. PARK6-linked autosomal recessive early-onset parkinsonism in Asian. *Neurology*. 2004;63(8):1482-1485.
18. Abou-Sleiman PM, Healy DG, Quinn N, Lees AJ, Wood NW. The role of pathogenic DJ-1 mutations in Parkinson's disease. *Ann Neurol*. 2003;54(3):283-286.
19. Ibáñez P, De Michele G, Bonifati V, et al. Screening for DJ-1 mutations in early onset autosomal recessive parkinsonism. *Neurology*. 2003;61(10):1429-1431.
20. Ibáñez P, Lesage S, Lohmann E, et al. Mutational analysis of the PINK1 gene in early-onset parkinsonism in Europe and North Africa. *Brain*. 2006;129(pt 3):686-694.
21. Valente EM, Salvi S, Ialongo T, et al. PINK1 mutations are associated with sporadic early-onset parkinsonism. *Ann Neurol*. 2004;56(3):336-341.
22. Abou-Sleiman PM, Muqit M, McDonald N, et al. A heterozygous effect for PINK1 mutations in Parkinson's disease? *Ann Neurol*. 2006;60(4):414-419.
23. Rogaeva E, Johnson J, Lang AE, et al. Analysis of the PINK1 gene in a large cohort of cases with Parkinson disease. *Arch Neurol*. 2004;61(12):1898-1904.
24. Khan NL, Valente EM, Bentivoglio AR, et al. Clinical and subclinical dopaminergic dysfunction in PARK6-linked parkinsonism: an 18F-dopa PET study. *Ann Neurol*. 2002;52(6):849-853.
25. Orimo S, Ozawa E, Nakade S, Sugimoto T, Mizusawa H. ^{123}I-metaiodobenzylguanidine myocardial scintigraphy in Parkinson's disease. *J Neurol Neurosurg Psychiatry*. 1999;67(2):189-194.
26. Orimo S, Amino T, Itoh Y, et al. Cardiac sympathetic denervation precedes neuronal loss in the sympathetic ganglia in Lewy body disease. *Acta Neuropathol*. 2005;109(6):583-588.
27. Suzuki M, Hattori N, Orimo S, et al. Preserved myocardial [^{123}I]metaiodobenzylguanidine uptake in autosomal recessive juvenile parkinsonism: first case report. *Mov Disord*. 2005;20(5):634-636.
28. Kitami T, Nomoto T, Nagao T, et al. ^{123}I-MIBG myocardial scintigraphy in juvenile parkinsonism. *Mov Disord*. 1998;13(suppl 2):247.
29. Orimo S, Amino T, Yokochi M, et al. Preserved cardiac sympathetic nerve accounts for normal cardiac uptake of MIBG in PARK2. *Mov Disord*. 2005;20(10):1350-1353.
30. Nagayama H, Hamamoto M, Ueda M, Nagashima J, Katayama Y. Reliability of MIBG myocardial scintigraphy in the diagnosis of Parkinson's disease. *J Neurol Neurosurg Psychiatry*. 2005;76(2):249-251.
31. Albanese A, Valente EM, Romito LM, Bellacchio E, Elia AE, Dallapiccola B. The PINK1 phenotype can be indistinguishable from idiopathic Parkinson disease. *Neurology*. 2005;64(11):1958-1960.
32. Pramstaller PP, Schlossmacher MG, Jacques TS, et al. Lewy body Parkinson's disease in a large pedigree with 77 Parkin mutation carriers. *Ann Neurol*. 2005;58(3):411-422.

Neuroscience Letters 449 (2009) 87–92

Contents lists available at ScienceDirect

Neuroscience Letters

journal homepage: www.elsevier.com/locate/neulet

Delivery of the aggregate inhibitor peptide QBP1 into the mouse brain using PTDs and its therapeutic effect on polyglutamine disease mice

H. Akiko Popiel, Yoshitaka Nagai *, Nobuhiro Fujikake, Tatsushi Toda

Division of Clinical Genetics, Department of Medical Genetics, Osaka University Graduate School of Medicine, 2-2-B9 Yamadaoka, Suita, Osaka 565-0871, Japan

ARTICLE INFO

Article history:
Received 3 April 2008
Received in revised form 12 May 2008
Accepted 5 June 2008

Keywords:
Protein transduction domain
Antennapedia
TAT
Aggregate inhibitor
Neurodegeneration
Polyglutamine
Huntington disease

ABSTRACT

The polyglutamine (polyQ) diseases are neurodegenerative diseases caused by proteins with an abnormally expanded polyQ stretch, which triggers abnormal aggregation of these proteins in the brain. We previously showed that the polyQ-binding peptide QBP1 inhibits polyQ aggregation, and further that administration of QBP1 fused with a protein transduction domain (PTD) suppresses polyQ-induced neurodegeneration in *Drosophila*. As the next step towards developing a therapy using QBP1, we investigated the delivery of PTD-QBP1 to the mouse brain upon its administration. Here we successfully detected delivery of PTD-QBP1 into mouse brain cells upon its single intracerebroventricular injection. In addition, long-term administration of PTD-QBP1 to polyQ disease mice improved their weight loss phenotype, suggesting a possible therapeutic effect. Our study indicates the potential of PTD-mediated delivery of QBP1 as a therapeutic strategy for the currently untreatable polyQ diseases.

The abnormal aggregation and deposition of misfolded proteins in the brain has recently been shown to be a common molecular mechanism involved in a wide range of neurodegenerative diseases such as Alzheimer disease, Parkinson disease, and the polyglutamine (polyQ) diseases [16]. The polyQ diseases, including Huntington disease and various types of spinocerebellar ataxia, are caused by a common mutation of an abnormal CAG repeat expansion in each unrelated disease-causing gene, which is translated into an expanded polyQ stretch in each unrelated disease-causing protein [12]. These proteins with an expanded polyQ stretch are thought to exert neurotoxicity via an initial change in their conformation, leading to their oligomerization and aggregation, and their eventual deposition as inclusion bodies within neurons [10,16,19,21]. There are currently no effective therapies for the polyQ diseases.

Based on the hypothesis that molecules that selectively bind to abnormally expanded polyQ stretches would inhibit their toxic properties, we identified polyQ-binding peptide 1 (QBP1; SNWKWWPGIFD) by combinatorial peptide library screening [11]. We recently showed that QBP1 indeed inhibits the toxic conformational transition of the expanded polyQ protein as well as its subsequent oligomer formation, indicating that QBP1 is an ideal therapeutic molecule since it targets the most initial change that occurs during the disease process [10,21]. We also showed that the genetic expression of QBP1 by a transgenic approach inhibits polyQ-induced neurodegeneration in a *Drosophila* model of the polyQ diseases, demonstrating its effectiveness *in vivo* [9]. Furthermore, towards the development of QBP1 as a therapeutic molecule that can exert its effects upon administration, we designed QBP1 fused with protein transduction domains (PTDs), which deliver covalently bound therapeutic cargo into cells [7,22], and showed that PTD-QBP1 suppresses polyQ-induced neurodegeneration in *Drosophila* [14].

As the next step towards developing a therapy using QBP1, it is important to determine the therapeutic effect of PTD-QBP1 administration on a mammalian model of the polyQ diseases. In this study we therefore investigated the delivery of PTD-QBP1 to the mouse brain upon its administration.

The following synthetic peptides were purchased from the University of North Carolina at Chapel Hill Peptide Synthesis Facility (Chapel Hill, NC): QBP1 (minimal active sequence [15]), WKWWPGIF; Antp-QBP1, GGRQIKIWFQNRRMKWKKGGWKWWPGIF; TAT-QBP1, GGGGYGRKKRRQRRRGGWKWWPGIF; and Antp-SCR, GGRQIKIWFQNRRMKWKKGGWPIWKGWF. All peptides were biotinylated at the N-terminus and amidated at the C-terminus.

Mice transgenic for human *huntingtin* exon 1 (strain R6/2) [8] were used. For single intraperitoneal (ip) injection of peptides, 500 μg of Antp-QBP1 or TAT-QBP1 (1 μg/μl in saline) was injected into the abdominal cavity of adult C57BL/6J mice. For intracarotid arterial injection of peptides, 500 μg of Antp-QBP1 or TAT-QBP1

* Corresponding author. Tel.: +81 6 6879 3381; fax: +81 6 6879 3389.
E-mail address: nagai@clgene.med.osaka-u.ac.jp (Y. Nagai).

0304-3940/$ – see front matter © 2008 Elsevier Ireland Ltd. All rights reserved.
doi:10.1016/j.neulet.2008.06.015

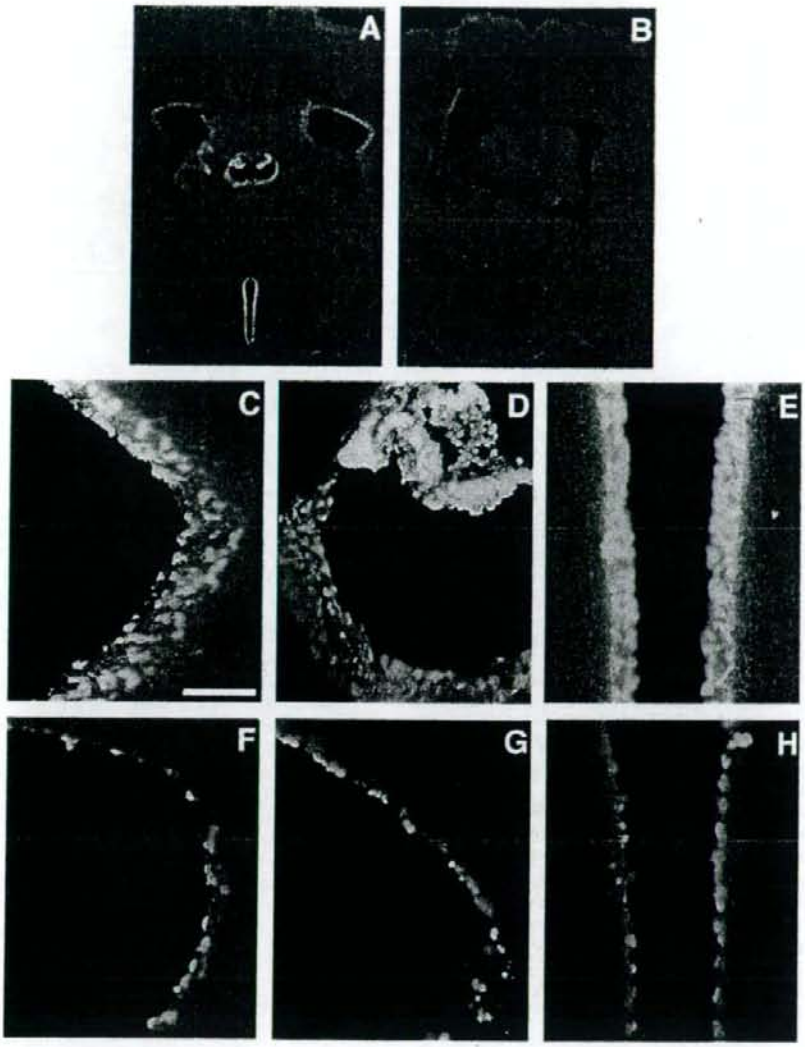

Fig. 1. Delivery of PTD-QBP1 into mouse brain cells upon icv injection. WT mice were given an icv injection of either biotin-tagged Antp-QBP1 (A, C–E, G, H), QBP1 (B), or TAT-QBP1 (F) (5 μg each), and 3 h (A–F) or 24 h later (G and H) brain sections were immunostained for the peptides. (A, B) Antp-QBP1 (A), but not QBP1 alone (B) is delivered into cells around all of the ventricles upon icv injection. (C–E) Higher magnification images of a part of the lateral ventricle (C), dorsal third ventricle (D), and third ventricle (E) shown in (A). Antp-QBP1 was delivered into numerous cells up to a few cell layers in depth around the ventricles. (F) TAT-QBP1 is also delivered into cells around the ventricles upon icv injection. Part of a lateral ventricle is shown. (G and H) Antp-QBP1 can still be detected within cells 24 h after injection. Part of a lateral ventricle (G) and third ventricle (H) is shown. Scale bar in (C) = 100 μm, and also applies to (D–H).

(5 μg/μl in 10% glycerol) was injected into the common carotid artery via a catheter into C57BL/6J mice. For single intracerebroventricular (icv) injection of peptides, 5 μg of QBP1, Antp-QBP1, or TAT-QBP1 (1 μg/μl) was stereotaxically injected into the right lateral ventricle (coordinates 1 mm right lateral to bregma and 3.5 mm ventral to the skull surface) of C57BL/6J mice using a 10 μl Hamilton syringe (Hamilton Company, Reno, NV), at a rate of 1 μl/min. QBP1 and TAT-QBP1 were dissolved in dimethyl sulfoxide due to their poor solubility in saline. For intrastriatal injection of peptides, 2 μg of Antp-QBP1 (1 μg/μl) was stereotaxically injected into the right striatum (coordinates 0.9 mm rostral to bregma, 2.0 mm right lateral to the midline and 3.2 mm ventral to the skull surface) of C57BL/6J mice.

For the therapeutic trials by continuous icv infusion of peptides to R6/2 mice, Antp-QBP1 was administered into the right lateral ventricle at a rate of 100 μg/week using an osmotic pump (DURECT, Cupertino, CA), from 4 weeks of age. For the therapeutic trials by long-term ip administration of peptides to R6/2 mice, Antp-QBP1 or saline was injected every other day (a total of 0.5 mg/week) to male mice from 4 weeks of age, and their

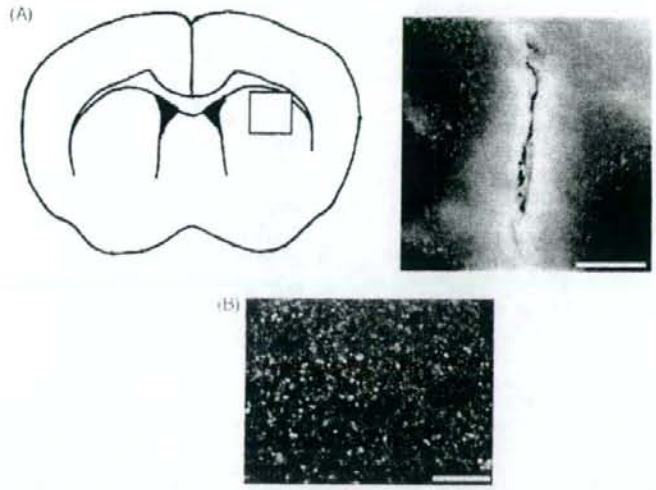

Fig. 2. Delivery of Antp-QBP1 into the mouse brain upon intrastriatal injection. Biotin-tagged Antp-QBP1 (2 μg) was injected into the striatum of a WT mouse brain, and 3 h later brain sections were immunostained for the peptide (green). (A) The left panel is a diagram of a mouse brain section, in which the box indicates the approximate area shown in the right panel. The asterisk indicates the needle tract, and scale bar = 250 μm. (B) Antp-QBP1 localization analyzed by confocal laser scanning microscopy. Cell nuclei were visualized by DAPI staining (blue). Scale bar = 10 μm. (For interpretation of the references to color in this figure legend, the reader is referred to the web version of the article.)

phenotypes were analyzed. For immunohistochemical analysis, Antp-QBP1 or Antp-SCR was intraperitoneally injected every day (a total of 2 mg/week) to male R6/2 mice from 2 weeks of age.

For rotarod analysis, mice were placed on a rotarod (Muromachi Kikai, Tokyo, Japan) revolving at 16 rpm. Mice were weighed weekly, and their lifespans were recorded.

For tissue preparation and immunohistochemistry, mouse brains were fixed with 4% paraformaldehyde in phosphate-buffered saline (PBS), and frozen coronal sections were cut. Sections were blocked in PBS containing 5% goat serum and 0.2% Triton X-100 for 1 h at room temperature, and then incubated with a goat anti-biotin antibody (1:2000; Sigma–Aldrich, St. Louis, MO) or a mouse anti-huntingtin antibody (1:200; MAB5374, Millipore, Billerica, MA) overnight at 4 °C, followed by an Alexa Fluor 488-conjugated rabbit anti-goat IgG antibody or an Alexa Fluor 546-conjugated goat anti-mouse IgG antibody (1:2000; Invitrogen, Carlsbad, CA), respectively, for 1 h at room temperature.

We first attempted to confirm the delivery of PTD-QBP1 into the mouse brain upon its administration. Since various studies have shown that ip injection of therapeutic peptides/proteins fused with a PTD results in their efficient delivery to the brain leading to therapeutic effects [1], we first tested ip injection of PTD-QBP1. QBP1 fused with Antp (Antp-QBP1, 500 μg), a PTD sequence derived from *Drosophila* Antennapedia [7], was injected intraperitoneally to wild type (WT) C57BL/6J mice, and 3 h later brain sections were immunostained for Antp-QBP1. However, we were unable to detect Antp-QBP1 in the brains of these mice (data not shown). Since the efficiency of delivery of a cargo molecule may depend on the type of PTD [17], we also used TAT, derived from human immunodefi-

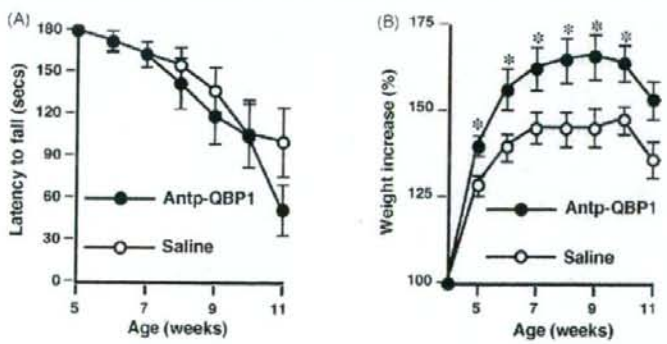

Fig. 3. Administration of Antp-QBP1 ameliorates the weight loss phenotype of polyQ disease mice. R6/2 mice were given ip injections of Antp-QBP1 (0.5 mg/week) or saline as a control from 4 weeks of age, and rotarod performance (A) and body weight (B) were measured weekly. Data in (B) are shown as percentage weight increase, in which the weight of each mouse at 4 weeks of age was counted as 100%. Values represent mean ± S.E.M., $n \geq 6$ mice per time point. *$P < 0.05$ (Student's *t*-test). Antp-QBP1 administration did not show any improvement in rotarod performance, but significantly ameliorated the weight loss of polyQ disease mice.

ciency virus-1, fused to QBP1 (TAT-QBP1) [22], but again could not detect delivery of the peptide into the brain (data not shown). We next injected Antp-QBP1 and TAT-QBP1 (500 μg) into the carotid artery which goes directly to the brain, since the peptides become very diluted upon ip injection. However, the peptides still could not be detected in the brains of these mice (data not shown). Lack of detection of the PTD-QBP1 peptides in the brain could be explained by the following reasons: (1) the peptides do not efficiently cross the blood–brain barrier (BBB), (2) the peptides are rapidly degraded, or (3) the peptides enter the cells in the brain but cannot be detected due to limited sensitivity of the immunohistochemical detection.

To determine whether PTD-QBP1 can be delivered efficiently into brain cells if the BBB is bypassed, we next tested direct administration of PTD-QBP1 into the mouse brain. Antp-QBP1 or QBP1 alone was injected into the right lateral ventricle of WT mice, 3 h later the brains were collected, and brain sections were immunostained for the peptides. Only Antp-QBP1, but not QBP1 alone, was delivered into brain cells not only around the injected ventricle but around all of the ventricles (Fig. 1A and B). Higher magnification revealed that the delivery of Antp-QBP1 was into numerous cells up to a few cell layers in depth around the ventricles (Fig. 1C–E). Icv injection of TAT-QBP1 also resulted in delivery of the peptide into brain cells, although it appeared less efficient than Antp-QBP1, and was observed in fewer cells in only a single cell layer around the ventricles (Fig. 1F). Taken together, these results indicate that PTD-QBP1, by virtue of the PTD, indeed has the ability to enter cells in the brain.

For PTD-QBP1 to be useful as a therapeutic molecule, it should be relatively stable, and not rapidly degraded. We therefore next analyzed the stability of Antp-QBP1 by waiting for 24 h after icv injection before collecting the brains. Antp-QBP1 was clearly detected within many cells around the ventricles even after 24 h (Fig. 1G and H). Since the cerebrospinal fluid (CSF) is rapidly turned over (every 4–5 h), this result indicates that Antp-QBP1 remained stable inside the cells rather than within the CSF. There could be some degradation, however, since Antp-QBP1 was present in fewer cells in only a single cell layer at 24 h after the injection (Fig. 1G and H) compared with the brain sections at 3 h (Fig. 1C–E). Therefore, these results demonstrate that Antp-QBP1 is relatively stable upon internalization into brain cells.

Our above results showed that upon icv injection, Antp-QBP1 is delivered into cells around the ventricles, but does not reach neurons further within the brain parenchyma. This is probably because icv injection relies on the free diffusion of Antp-QBP1 from the ventricular space into the brain parenchyma for its spread, and because the ependymal cells which line the ventricles may interfere with this free diffusion. We therefore next analyzed whether injecting Antp-QBP1 directly into the brain parenchyma would lead to more widespread delivery of the peptide into neurons in the brain. Antp-QBP1 was injected into the right striatum of WT mice, and 3 h later brain sections were immunostained for Antp-QBP1. Intrastriatal injection resulted in more spread of the peptide compared with icv injection (Fig. 2A), probably due to bypass of the ependymal cell barrier. However, Antp-QBP1 still did not widely spread into cells throughout the brain. We further analyzed the brain sections by confocal laser scanning microscopy to examine whether Antp-QBP1 is actually being delivered into cells. Antp-QBP1 appeared to be present around the injection area, including immediately around the cell nuclei, and was not excluded from the cell bodies (Fig. 2B). This suggests that at least some of the injected peptide is actually being delivered into the brain cells upon intrastriatal injection.

We next tested the therapeutic effects of Antp-QBP1 administration on the neurodegenerative phenotypes of polyQ disease mice. We utilized the R6/2 Huntington disease mouse model which is transgenic for exon 1 of the human *huntingtin* gene with approximately 150 CAG repeats [8]. Since we successfully detected the delivery of Antp-QBP1 into cells in a small area of the brain by icv injection, we first examined if continuous icv administration would lead to greater spread of the peptide throughout the brain and exert therapeutic effects. We therefore utilized osmotic pumps to continuously infuse Antp-QBP1 (100 μg/week) into the lateral ventricle of R6/2 mice from 4 weeks of age. However, since implantation of the osmotic pump itself affected the phenotype of the mice, we were unable to adequately assess the therapeutic effect of Antp-QBP1. Furthermore, immunohistochemical analysis revealed that Antp-QBP1 did not spread greatly throughout the brain even upon its continuous icv infusion (data not shown) compared to its single icv injection, probably due to the limited diffusion from the ventricular space as well as the presence of the ependymal cells.

We therefore next tested long-term ip administration of Antp-QBP1, since it is a much less invasive method as compared to continuous icv infusion using implanted osmotic pumps. Furthermore, since ip injection relies on the bloodstream for the spread of Antp-QBP1, and virtually every neuron in the brain is perfused by its own blood vessel [13], this method can potentially lead to widespread delivery of the peptide throughout the brain. R6/2 mice were given ip injections of either Antp-QBP1 or saline as a control from 4 weeks of age, and its therapeutic effects on impaired

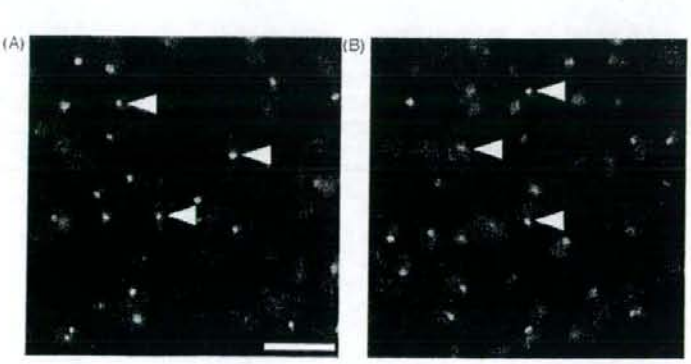

Fig. 4. Effect of Antp-QBP1 administration on htt inclusion body formation in the brains of polyQ disease mice. R6/2 mice were given ip injections of Antp-QBP1 (2 mg/week) (A) or Antp-SCR (B) as a control from 2 weeks of age, brains were collected at 11 weeks of age and brain sections were immunostained with an anti-htt antibody to detect inclusion bodies (arrowheads). Scale bar = 25 μm. Antp-QBP1 treatment did not result in an obvious decrease in htt inclusion body formation.

rotarod performance, weight loss, and shortened lifespan, which are caused by polyQ-induced neurodegeneration, were analyzed. At 5 weeks of age, R6/2 mice of both treatment groups remained on the rotarod for the whole testing period (180 s), and performed similarly to WT mice as reported previously [6] (Fig. 3A). The average time on the rotarod decreased similarly in both treatment groups with age, indicating that Antp-QBP1 administration does not ameliorate the impairment of rotarod performance of these mice. We also analyzed the therapeutic effect of Antp-QBP1 on the weight loss of these mice, by evaluating their weight increase from 5 weeks of age. The increase in weight of R6/2 mice stops around 6 weeks of age, and they begin to lose weight from around 10 weeks of age, while their WT littermates continue to gain weight [3] (Fig. 3B). Antp-QBP1 treated R6/2 mice showed a significant improvement in weight increase compared to saline treated mice from 5 to 10 weeks of age, suggesting a possible therapeutic effect. The average lifespan of Antp-QBP1 treated R6/2 mice was not significantly different from that of saline treated mice (91.7 ± 6.8 days vs. 104.4 ± 5.1 days, respectively).

We further analyzed whether Antp-QBP1 treatment had any effects on inclusion body formation of the polyQ-expanded huntingtin (htt) protein in R6/2 mouse brains, by immunohistochemistry. Mice were treated from 2 weeks of age, brains were collected at 11 weeks of age, and brain sections were immunostained with an anti-htt antibody. The intranuclear htt inclusion bodies formed in the neurons of R6/2 mice were clearly detected by the anti-htt antibody (Fig. 4). However, there was no obvious difference in inclusion body formation between mice treated with Antp-QBP1 and Antp-SCR (a scrambled sequence of QBP1 fused with Antp), used as a control. The fact that a therapeutic effect was only observed against the weight loss phenotype is likely to be due to the low efficiency of Antp-QBP1 delivery to the brain. Another possibility is that since R6/2 mice exhibit very severe disease phenotypes [6], it might be difficult to significantly modify the phenotypes by this treatment.

In this paper we demonstrate that the aggregate inhibitor peptide QBP1 can be delivered into cells of the mammalian brain upon its administration, by addition of a PTD. In addition, we found that long-term ip administration of Antp-QBP1 to a mouse model of the polyQ diseases ameliorated its weight loss phenotype. This suggests the possibility that a small amount of Antp-QBP1 is crossing the BBB and entering neurons, to exert its therapeutic effect. Although we could not detect the delivery of Antp-QBP1 into the mouse brain by ip injection, this could be due to the limited sensitivity of immunohistochemical detection. In fact, in our previous study using a *Drosophila* model of the polyQ diseases, the internalized Antp-QBP1 in the brain also could not be detected, but we still observed its therapeutic effect on neurological phenotypes [14]. However, we cannot exclude the possibility that Antp-QBP1 is acting at the periphery to ameliorate the weight loss of polyQ disease mice.

In the future, to maximize the therapeutic effect of QBP1 treatment, methods to improve the efficiency of Antp-QBP1 delivery to the brain should be investigated. Notably, a recent study reported a short secretory signal that is adjacent to the Antp sequence in the full-length *Drosophila* Antennapedia, which enables the secretion of Antp after its internalization into cells [4]. Addition of such a sequence should enable the secretion of Antp-QBP1 from the cells it first enters, thus allowing its repeated internalization and secretion, which should improve its spread throughout the brain parenchyma and/or its delivery across the BBB. In addition, preincubation with negatively charged sugars such as α-2,8-polysialic acid has been reported to enhance the diffusion of PTDs [18], and may also improve the spread of Antp-QBP1 throughout the brain.

Many other neurodegenerative diseases including Alzheimer disease and Parkinson disease are also caused by the abnormal aggregation of misfolded proteins in the brain [16], and peptides/proteins that inhibit their aggregation and exert therapeutic effects have been reported [2,5,20]. Although the clinical application of these aggregate inhibitor peptides/proteins in human patients has been greatly anticipated, the lack of a method for their safe and efficient delivery into the brain has been a major obstacle. Our study therefore indicates the great potential of PTD-mediated delivery of aggregate inhibitor peptides/proteins into the brain, as a general therapeutic strategy for neurodegenerative diseases involving abnormal protein aggregation.

Acknowledgements

We thank J.T. Pearson and M. Shirai for assistance with the mouse experiments. This work was supported in part by Grants-in-Aid for Scientific Research on Priority Areas (to Y.N.; Advanced Brain Science Project, Research on Pathomechanisms of Brain Disorders, Life of Proteins, and Water and Biomolecules) from MEXT, Japan; by a Grant-in-Aid for the Research Committee for Ataxic Diseases (to Y.N.) from the Ministry of Health, Labor, and Welfare, Japan; and by a Scholarship for Foreign Nationals in Japan (to H.A.P.) from the Ichiro Kanehara Foundation, Japan.

References

[1] S. Asoh, I. Ohsawa, T. Mori, K. Katsura, T. Hiraide, Y. Katayama, M. Kimura, D. Ozaki, K. Yamagata, S. Ohta, Protection against ischemic brain injury by protein therapeutics, Proc. Natl. Acad. Sci. U.S.A. 99 (2002) 17107–17112.
[2] A.M. Bodles, O.M. El-Agnaf, B. Greer, D.J. Guthrie, G.B. Irvine, Inhibition of fibril formation and toxicity of a fragment of α-synuclein by an *N*-methylated peptide analogue, Neurosci. Lett. 359 (2004) 89–93.
[3] S.W. Davies, M. Turmaine, B.A. Cozens, M. DiFiglia, A.H. Sharp, C.A. Ross, E. Scherzinger, E.E. Wanker, L. Mangiarini, G.P. Bates, Formation of neuronal intranuclear inclusions underlies the neurological dysfunction in mice transgenic for the HD mutation, Cell 90 (1997) 537–548.
[4] E. Dupont, A. Prochiantz, A. Joliot, Identification of a signal peptide for unconventional secretion, J. Biol. Chem. 282 (2007) 8994–9000.
[5] H. Hayashi, N. Kimura, H. Yamaguchi, K. Hasegawa, T. Yokoseki, M. Shibata, N. Yamamoto, M. Michikawa, Y. Yoshikawa, K. Terao, K. Matsuzaki, C.A. Lemere, D.J. Selkoe, H. Naiki, K. Yanagisawa, A seed for Alzheimer amyloid in the brain, J. Neurosci. 24 (2004) 4894–4902.
[6] M.A. Hickey, K. Gallant, G.G. Gross, M.S. Levine, M.F. Chesselet, Early behavioural deficits in R6/2 mice suitable for use in preclinical drug testing, Neurobiol. Dis. 20 (2005) 1–11.
[7] A. Joliot, A. Prochiantz, Transduction peptides: from technology to physiology, Nat. Cell Biol. 6 (2004) 189–196.
[8] L. Mangiarini, K. Sathasivam, M. Seller, B. Cozens, A. Harper, C. Hetherington, M. Lawton, Y. Trottier, H. Lehrach, S.W. Davies, G.P. Bates, Exon 1 of the *HD* gene with an expanded CAG repeat is sufficient to cause a progressive neurological phenotype in transgenic mice, Cell 87 (1996) 493–506.
[9] Y. Nagai, N. Fujikake, K. Ohno, H. Higashiyama, H.A. Popiel, J. Rahadian, M. Yamaguchi, W.J. Strittmatter, J.R. Burke, T. Toda, Prevention of polyglutamine oligomerization and neurodegeneration by the peptide inhibitor QBP1 in *Drosophila*, Hum. Mol. Genet. 12 (2003) 1253–1259.
[10] Y. Nagai, T. Inui, H.A. Popiel, N. Fujikake, K. Hasegawa, Y. Urade, Y. Goto, H. Naiki, T. Toda, A toxic monomeric conformer of the polyglutamine protein, Nat. Struct. Mol. Biol. 14 (2007) 332–340.
[11] Y. Nagai, T. Tucker, H. Ren, D.J. Kenan, B.S. Henderson, J.D. Keene, W.J. Strittmatter, J.R. Burke, Inhibition of polyglutamine protein aggregation and cell death by novel peptides identified by phage display screening, J. Biol. Chem. 275 (2000) 10437–10442.
[12] H.T. Orr, H.Y. Zoghbi, Trinucleotide repeat disorders, Annu. Rev. Neurosci. 30 (2007) 575–621.
[13] W.M. Pardridge, Drug and gene delivery to the brain: the vascular route, Neuron 36 (2002) 555–558.
[14] H.A. Popiel, Y. Nagai, N. Fujikake, T. Toda, Protein transduction domain-mediated delivery of QBP1 suppresses polyglutamine-induced neurodegeneration *in vivo*, Mol. Ther. 15 (2007) 303–309.
[15] H. Ren, Y. Nagai, T. Tucker, W.J. Strittmatter, J.R. Burke, Amino acid sequence requirements of peptides that inhibit polyglutamine–protein aggregation and cell death, Biochem. Biophys. Res. Commun. 288 (2001) 703–710.
[16] C.A. Ross, M.A. Poirier, Protein aggregation and neurodegenerative disease, Nat. Med. 10 (Suppl.) (2004) S10–S17.

[17] P. Saalik, A. Elmquist, M. Hansen, K. Padari, K. Saar, K. Viht, U. Langel, M. Pooga, Protein cargo delivery properties of cell-penetrating peptides. A comparative study, Bioconjug. Chem. 15 (2004) 1246–1253.
[18] M.P. Schutze-Redelmeier, H. Gournier, F. Garcia-Pons, M. Moussa, A.H. Joliot, M. Volovitch, A. Prochiantz, F.A. Lemonnier, Introduction of exogenous antigens into the MHC class I processing and presentation pathway by *Drosophila* Antennapedia homeodomain primes cytotoxic T cells in vivo, J. Immunol. 157 (1996) 650–655.
[19] J. Shao, M.I. Diamond, Polyglutamine diseases: emerging concepts in pathogenesis and therapy, Hum. Mol. Genet. 16 (Spec. No. 2) (2007) R115–R123.
[20] C. Soto, E.M. Sigurdsson, L. Morelli, R.A. Kumar, E.M. Castano, B. Frangione, β-Sheet breaker peptides inhibit fibrillogenesis in a rat brain model of amyloidosis: implications for Alzheimer's therapy, Nat. Med. 4 (1998) 822–826.
[21] Y. Takahashi, Y. Okamoto, H.A. Popiel, N. Fujikake, T. Toda, M. Kinjo, Y. Nagai, Detection of polyglutamine protein oligomers in cells by fluorescence correlation spectroscopy, J. Biol. Chem. 282 (2007) 24039–24048.
[22] J.S. Wadia, S.F. Dowdy, Protein transduction technology, Curr. Opin. Biotechnol. 13 (2002) 52–56.

Human Molecular Genetics, 2009, Vol. 18, No. 4 **621–631**
doi:10.1093/hmg/ddn387
Advance Access published on November 18, 2008

Residual laminin-binding activity and enhanced dystroglycan glycosylation by LARGE in novel model mice to dystroglycanopathy

Motoi Kanagawa[1,†], Akemi Nishimoto[1,†], Tomohiro Chiyonobu[1], Satoshi Takeda[3], Yuko Miyagoe-Suzuki[4], Fan Wang[1], Nobuhiro Fujikake[1], Mariko Taniguchi[1], Zhongpeng Lu[1], Masaji Tachikawa[1], Yoshitaka Nagai[1], Fumi Tashiro[2], Jun-Ichi Miyazaki[2], Youichi Tajima[5], Shin'ichi Takeda[4], Tamao Endo[6], Kazuhiro Kobayashi[1], Kevin P. Campbell[7,8,9,10,11] and Tatsushi Toda[1,*]

[1]Division of Clinical Genetics, Department of Medical Genetics and [2]Division of Stem Cell Regulation Research, Department of Molecular Therapeutics, Osaka University Graduate School of Medicine, Suita, Osaka 565-0871, Japan, [3]Otsuka GEN Research Institute, Otsuka Pharmaceutical Co. Ltd, Tokushima 771-0192, Japan, [4]Department of Molecular Therapy, National Institute of Neuroscience, National Center of Neurology and Psychiatry, 4-1-1 Ogawa-higashi, Kodaira, Tokyo 187-8502, Japan, [5]Department of Clinical Genetics, The Tokyo Metropolitan Institute of Medical Science, Tokyo Metropolitan Organization for Medical Research, 3-18-22 Honkomagome, Bunkyo-ku, Tokyo 113-8613, Japan, [6]Glycobiology Research Group, Tokyo Metropolitan Institute of Gerontology, Foundation for Research on Aging and Promotion of Human Welfare, 35-2 Sakaecho, Itabashi-ku, Tokyo 173-0015, Japan, [7]Howard Hughes Medical Institute, [8]Senator Paul D. Wellstone Muscular Dystrophy Cooperative Research Center, [9]Department of Molecular Physiology and Biophysics, [10]Department of Neurology and [11]Department of Internal Medicine, Roy J. and Lucille A. Carver College of Medicine, The University of Iowa, Iowa City, IA 52242, USA

Received July 21, 2008; Revised November 2, 2008; Accepted November 12, 2008

Hypoglycosylation and reduced laminin-binding activity of α-dystroglycan are common characteristics of dystroglycanopathy, which is a group of congenital and limb-girdle muscular dystrophies. Fukuyama-type congenital muscular dystrophy (FCMD), caused by a mutation in the *fukutin* gene, is a severe form of dystroglycanopathy. A retrotransposal insertion in *fukutin* is seen in almost all cases of FCMD. To better understand the molecular pathogenesis of dystroglycanopathies and to explore therapeutic strategies, we generated knock-in mice carrying the retrotransposal insertion in the mouse *fukutin* ortholog. Knock-in mice exhibited hypoglycosylated α-dystroglycan; however, no signs of muscular dystrophy were observed. More sensitive methods detected minor levels of intact α-dystroglycan, and solid-phase assays determined laminin binding levels to be ~50% of normal. In contrast, intact α-dystroglycan is undetectable in the dystrophic Large^{myd} mouse, and laminin-binding activity is markedly reduced. These data indicate that a small amount of intact α-dystroglycan is sufficient to maintain muscle cell integrity in knock-in mice, suggesting that the treatment of dystroglycanopathies might not require the full recovery of glycosylation. To examine whether glycosylation defects can be restored *in vivo*, we performed mouse gene transfer experiments. Transfer of *fukutin* into knock-in mice restored glycosylation of α-dystroglycan. In addition, transfer of *LARGE* produced laminin-binding forms of α-dystroglycan in both knock-in mice and the *POMGnT1* mutant mouse, which is another model of dystroglycanopathy. Overall, these data suggest that even

*To whom correspondence should be addressed at: Division of Clinical Genetics, Department of Medical Genetics, Osaka University Graduate School of Medicine, 2-2-B9, Yamadaoka, Suita 565-0871, Japan. Tel: +81 668793381; Fax: +81 668793389; Email: toda@clgene.med.osaka-u.ac.jp
†The authors wish it to be known that, in their opinion, the first two authors should be regarded as joint First Authors.

partial restoration of α-dystroglycan glycosylation and laminin-binding activity by replacing or augmenting glycosylation-related genes might effectively deter dystroglycanopathy progression and thus provide therapeutic benefits.

INTRODUCTION

Dystroglycanopathy is a group of congenital and limb-girdle muscular dystrophies that includes Walker–Warburg syndrome (WWS), muscle-eye-brain (MEB) disease, Fukuyama-type congenital muscular dystrophy (FCMD), congenital muscular dystrophy 1C/D (1,2) and limb-girdle muscular dystrophy (LGMD) 2I/K/M/N (3–6). Hypoglycosylation of α-dystroglycan is a hallmark of these disorders. So far, six genes (*POMT1*, *POMT2*, *POMGnT1*, *fukutin*, *FKRP* and *LARGE*) have been implicated in dystroglycanopathies and all are thought to be involved in glycosylation of α-dystroglycan. POMGnT1 and the POMT1/2 complexes are known to have glycosyltransferase activities that place *O*-mannosyl sugar chains on α-dystroglycan (7,8). The exact functions of fukutin, FKRP and LARGE are still unknown.

α-Dystroglycan (α-DG) is a receptor for laminin in the basement membrane and is anchored on the plasma membrane through non-covalent interaction with a transmembrane-type β-DG (9). α- and β-DGs are encoded by a single mRNA that is cleaved into two subunits during post-translational maturation. *O*-glycosylation of α-DG is required for ligand-binding activity. Although the exact binding epitope for ligand is still unknown, one unique *O*-mannosyl glycan [Neu5Ac(α2–3)Gal(β1–4)GlcNAc(β1–2)Man-Ser/Thr] (10) appears to be involved in ligand binding among extensive and heterogenous groups of *O*-linked sugar chains. β-DG interacts with dystrophin, which in turn binds to actin filaments. The DG complex spans the plasma membrane, connecting the basement membrane to the actin cytoskeleton and presumably conferring mechanical stability to muscle cells during muscle contraction.

In Japan, FCMD is the most common congenital muscular dystrophy and, following Duchenne muscular dystrophy, is the second most common childhood muscular dystrophy. An autosomal recessive disorder, FCMD is characterized by severe muscular dystrophy, abnormal neuronal migration associated with mental retardation and epilepsy and, frequently, eye abnormalities (11). A recent study revealed aberrant neuromuscular junction formation and delayed muscle terminal maturation in FCMD, suggesting that a maturational delay of muscle fibers underlies the etiology of FCMD (12). Through positional cloning we identified *fukutin*, the gene responsible for FCMD (13). The predominant mutation in FCMD was identified as a 3 kb SINE-VNTR-*Alu* (SVA) retrotransposon insertion into the 3′-UTR of *fukutin*. In Japan, 70–80% of FCMD patients are homozygous for this retrotransposal insertion. Compound heterozygosity, exhibiting both a retrotransposonal mutation and a point mutation, is sometimes seen and generally exhibits more severe pathologies (13–15). Only a few cases with non-founder mutations (homozygous for point mutations) have been reported outside of Japan (5,16–19).

MEB disease is a severe autosomal recessive disease, similar to FCMD, characterized by congenital muscular dystrophy, ocular abnormalities and brain malformation. The gene responsible for MEB is *POMGnT1*, which encodes protein *O*-linked mannose β1,2-*N*-acetylglucosaminyltransferase 1 (7). In both FCMD and MEB disease, α-DG glycosylation and laminin-binding activity are severely disrupted (20). The Large^{myd} mouse, a spontaneous mutant, has been used as a model for dystroglycanopathy. As is the case with human dystroglycanopathies, α-DG in Large^{myd} mice is hypoglycosylated and shows reduced ligand-binding activity (20,21). Positional cloning in this model identified a disease-causing mutation in the *Large* gene (22), which encodes a protein with a transmembrane domain followed by a coiled-coil domain and two DxD-containing putative catalytic domains (23). *LARGE* mutations are also seen in human dystroglycanopathy (24). Although the exact function of the LARGE protein is not fully understood, it has been shown to produce hyperglycosylated α-DG in culture cells and mice (25,26). In addition, physical interaction between LARGE and α-DG is an essential step in acquiring ligand-binding activities of α-DG (25). Therefore, it is believed that LARGE plays a post-translational role in modulating both α-DG glycosylation and its functional expression.

To further investigate molecular pathogenesis and to explore therapeutic strategies for dystroglycanopathy, we generated several model mice for FCMD. We first generated mice with a targeted *fukutin* disruption, but this model showed embryonic lethality (27). We also generated chimeric fukutin mice by injecting homozygous targeted (*fukutin*$^{-/-}$) ES cells into blastocysts (28). Mice with high chimerism showed dystrophic skeletal muscle; however, the variability of chimerism among individuals, and with growth, limits this experimental approach. Therefore, we generated a transgenic knock-in mouse model carrying the retrotransposal insertion in *fukutin*. Our data revealed that even a small amount of intact α-DG is sufficient to maintain skeletal muscle function, and suggest that increasing the expression of glycosylation-related genes, which could be accomplished through various approaches, can be a therapeutic strategy for preventing or slowing progression of a broad range of dystroglycanopathies.

RESULTS

Generation of model mice for FCMD

To generate a transgenic knock-in mouse carrying the retrotransposal insertion, we replaced mouse *fukutin* exon 10 with a FCMD patient's exon 10, engineered to contain the retrotransposal insertion using a site-directed DNA integration technique. Exon 10 encodes amino acids from Tyr-392 to the C-terminal end and the 3′-UTR. We also generated another transgene containing a normal human exon 10. The terms Hn (human normal; Fig. 1A, no. 6) and Hp (human patient; Fig. 1A, no. 7) refer to transgenes containing the normal human exon 10 and the patient's exon 10, respectively.

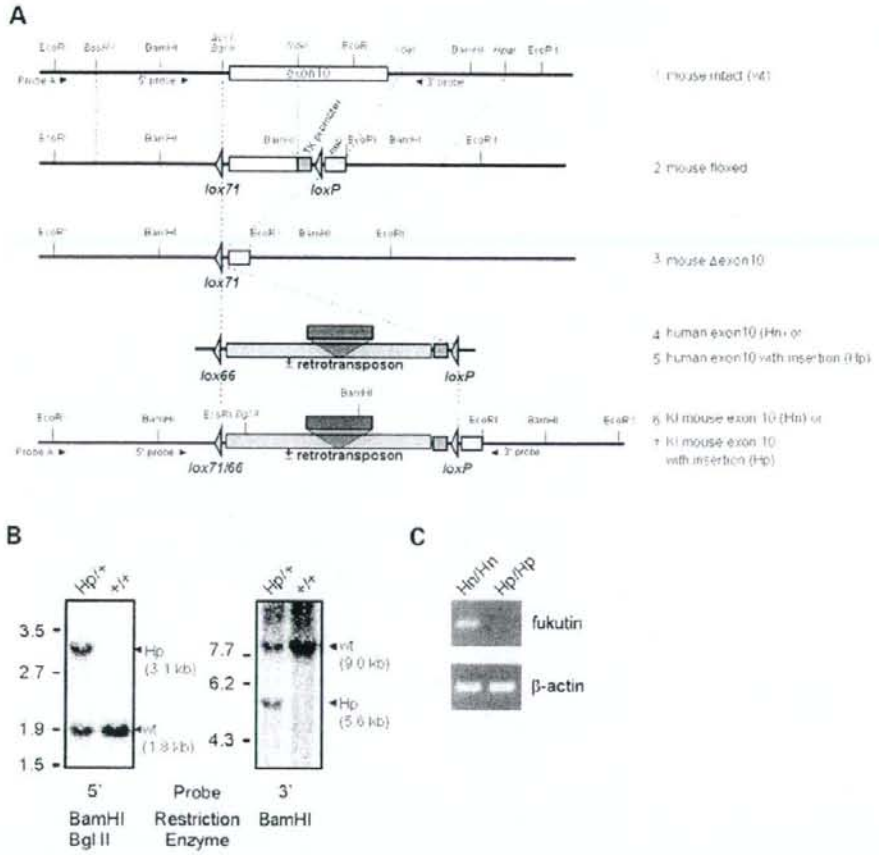

Figure 1. Generation of FCMD model mice that carry the retrotransposal insertion in the mouse *fukutin* gene. (**A**) Schematic representation of the targeting vector. Details are described in the Materials and Methods section. Human *fukutin* exon10 is shown in green, and the retrotransposon is shown in red. (**B**) Southern blot analysis of mouse genomic DNA. Insertion of the human exon10 with the retrotransposon yields new 3.1 kb BamHI/Bgl II and 5.6 kb fragments that hybridize, respectively, with the 5′ and 3′ probes shown in (A). (**C**) RT–PCR analysis. *fukutin* transcripts were amplified using RT-PCR. A β-actin internal control is shown (bottom panel).

Recombination was confirmed using Southern blot analysis of genomic DNA from ES cells (data not shown). Targeted ES cell clones were injected into blastocysts to obtain chimeric mice. Germline transmission of the knock-in allele was established via Southern blot analysis of mouse genomic DNA (Fig. 1B). Germline-competent heterozygous mice were in turn mated to generate homozygous mutants (Hn/Hn and Hp/Hp) (Fig. 2A, nos 3 and 4). RT–PCR showed a dramatic reduction of *fukutin* mRNA transcript levels in Hp/Hp mice (Fig. 1C). Through quantitative PCR, we determined that Hp/Hp mice express *fukutin* transcript at 5–10% of normal levels (data not shown). We consider Hp/Hp mice to be models for most FCMD cases that are homozygous for the retrotransposal insertion. Human patients who are compound heterozygous for the insertion and a nonsense *fukutin* mutation generally show more severe pathology than those who are homozygous for the insertion (14). Therefore, we crossed Hp/Hp mice with transgenic mice carrying a neo cassette disruption of one *fukutin* allele (fukutin$^{+/-}$) (27) to create a compound heterozygous line. The Hp/+ mice in this line represent retrotransposon carriers (Fig. 2A, no. 5) and the Hp/− mice represent compound heterozygotes (Fig. 2A, no. 6).

FCMD model mice exhibit hypoglycosylation of α-DG

To characterize the biochemical properties of α-DG in the knock-in mice, we prepared skeletal muscle samples enriched for α-DG with wheat germ agglutinin (WGA) beads, which is able to bind nearly all the DG in the muscle sample (20,29). These preparations were analyzed using western blot analysis with goat polyclonal antibodies against α-DG core protein (AP-074G-C) and the monoclonal antibody IIH6. IIH6 recognizes glycosylated epitopes on α-DG, and hypoglycosylation results in the absence of epitopes for the antibody (20).

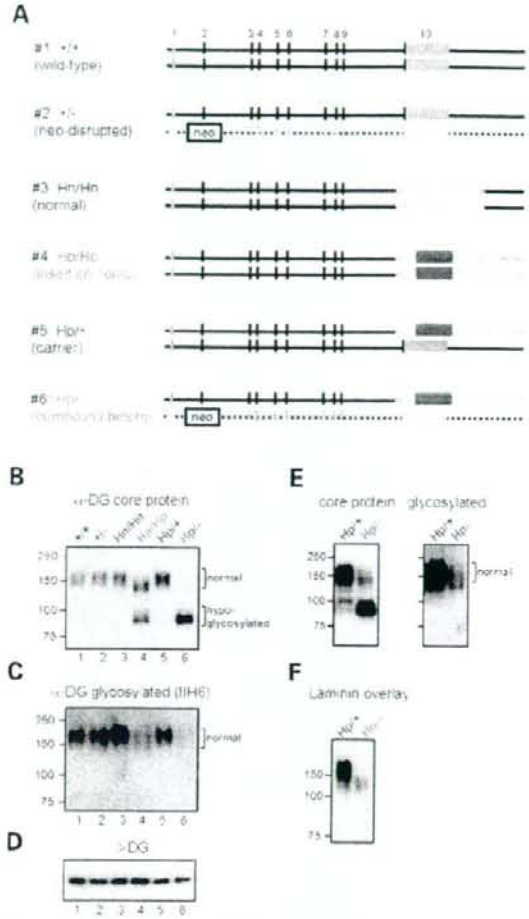

Figure 2. FCMD models exhibit hypoglycosylation and laminin-binding activity. (**A**) Schematic representation of the control and mutant *fukutin* genes in model mice. 1, wild-type mice (+/+); 2, mice carrying a neo-disrupted *fukutin* allele (+/−); 3, mice homozygous for the Hn allele (Hn/Hn); 4, mice homozygous for the Hp allele (Hp/Hp); 5, mice with a Hp allele and an intact mouse *fukutin* allele (Hp/+); and 6, mice with a Hp allele and a neo-disrupted allele (Hp/−). Exons are indicated with filled boxes. Portions derived from human *fukutin* exon 10 are shown in orange and green (3′-UTR). The retrotransposal insertion is shown in red. (**B–F**) Biochemical characterization of FCMD model mice. WGA beads were added to solubilized skeletal muscle samples to enrich DG from each model mouse. FCMD models are shown in red (Hp/Hp and Hp/−). WGA preparations were analyzed by western blot using antibodies against core protein (B) and glycosylated α-DG (C). The western blot for β-DG shows comparable amounts of DG proteins in each lane (D). Overexposure of blots analyzing core protein and glycosylated α-DG detected the presence of intact α-DG proteins in Hp/− mice (E). The portions of normal-sized and hypoglycosylated α-DGs are indicated at the right side of the blots. A laminin overlay assay was performed using samples from Hp/− mice and the litter control Hp/+ mice (F).

Western blot analysis of α-DG core protein revealed the presence of ∼150 kDa α-DG proteins in the control group (+/+, +/−, Hn/Hn and Hp/+ mice) (Fig. 2B, lanes 1–3 and 5). A slight reduction in molecular weight was observed in Hp/Hp mice (Fig. 2B, lane 4, upper band). In Hp/− mice, we observed a much-reduced intensity of the ∼150 kDa bands (Fig. 2B, lane 6). In addition, lower molecular weight (∼90 kDa) bands were detected in Hp/Hp and Hp/− mice (Fig. 2B, lanes 4 and 6). Western blotting with IIH6 detected ∼150 kDa bands in the control groups (+/+, +/−, Hn/Hn and Hp/+) (Fig. 2C, lanes 1–3 and 5). IIH6 reactivity at ∼150 kDa in Hp/Hp and Hp/− mice was reduced relative to controls (Fig. 2C, lanes 4 and 6). α-DG proteins with reduced molecular weight (∼90 kDa) were not recognized by IIH6, indicating that they are hypoglycosylated. Western blot analysis of β-DG confirmed comparable levels of DG proteins among the samples (Fig. 2D). Hp/− mice consistently contained more hypoglycosylated α-DG than Hp/Hp mice; therefore, we used Hp/− mice as models for FCMD and their Hp/+ littermates as controls. Longer exposure of blots from Hp/− mice detected an α-DG species recognized by IIH6 with the molecular weight of ∼150 kDa (Fig. 2E), suggesting that a small amount of intact α-DG also is present. Analysis of laminin-binding activity in Hp/− mice and Hp/+ littermates using a laminin overlay assay (Fig. 2F) showed reduced laminin-binding activity in Hp/− mice.

A small amount of intact α-DG prevents muscular dystrophy

We examined hematoxylin and eosin (H&E) stained sections of the quadriceps, gastrocnemius, tibialis anterior, soleus, iliopsoas and diaphragm muscles in Hp/+ and Hp/− mice. H&E staining revealed no clear difference between Hp/+ and Hp/− mice. Histopathological features of muscular dystrophy, such as centrally located nuclei, tissue fibrosis and fatty infiltration were not observed in 10-week-old FCMD models Hp/− (Fig. 3A) and Hp/Hp mice (data not shown). Although FCMD onset in humans occurs at or near birth, we also examined older mice to determine whether onset in Hp/− mice was delayed. Even in older mice (>1 year old), we observed no signs of muscular dystrophy (Fig. 3B). There was no obvious change in the expression level of laminin α2 chain, which is the major ligand of α-DG in the skeletal muscle (Supplementary Material, Fig. S1).

Both hypoglycosylated and IIH6-positive intact α-DG proteins were detected in Hp/Hp and Hp/− mouse brains (Supplementary Material, Fig. S2). As is the case with skeletal muscle, Hp/− mice contained more hypoglycosylated α-DG. Apparent brain histological abnormality was hardly detected in Hp/− mice; only a few mice showed a very small ectopic cluster of neurons migrating into the marginal zone. We also analyzed α-DG in heart, liver, and lung from Hp/− mice, and found that the levels of hypoglycosylation and laminin-binding activity vary between the tissues (less affected in heart and liver) (Supplementary Material, Figs S2 and S3).

To analyze potential weakness in muscle cell membrane integrity, which may not be detectable in housed mice by H&E staining, Hp/− mice were subjected to treadmill exercise followed by the measurement of Evans blue dye (EBD) incorporation into muscle fibers. EBD is a membrane-impermeant molecule that binds to serum albumin and is physically restricted from fibers unless the skeletal muscle membrane is damaged (30). Even after exercising to exhaustion, Hp/− mice showed no EBD uptake in muscle cells (data not shown).

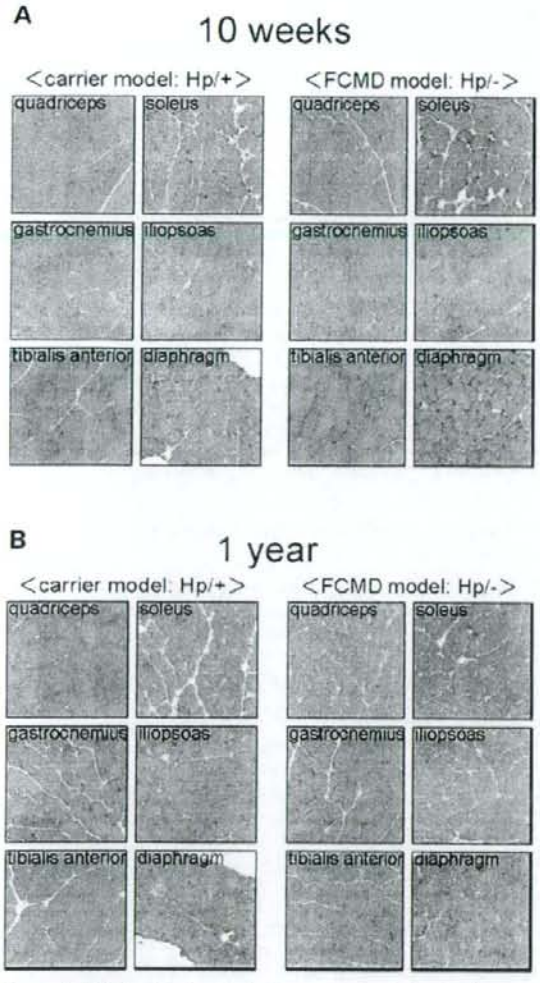

Figure 3. FCMD mice do not develop a muscular dystrophy phenotype. Various skeletal muscle tissues from Hp/− and littermate control Hp/+ mice at 10 weeks (**A**) and >1 year (**B**) of age were analyzed by H&E staining. No features of muscular dystrophy or other variation from controls were observed in Hp/− mice.

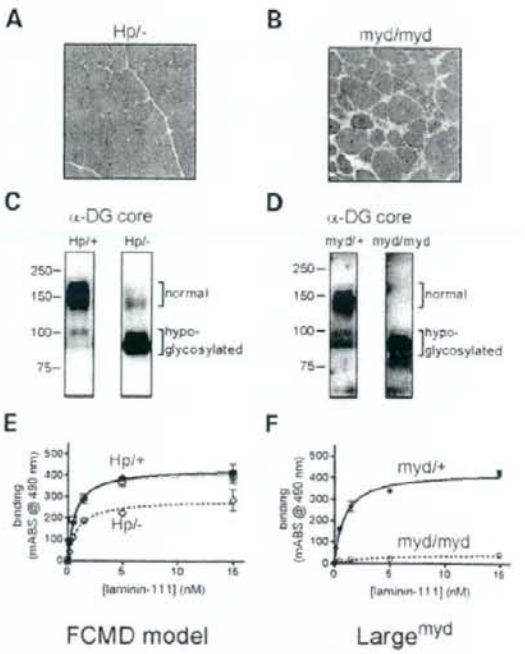

Figure 4. Laminin-binding activity is maintained in Hp/− mice but barely detected in Large^{myd} mice. H&E staining of quadriceps tissue from Hp/− (**A**) and Large^{myd} (myd/myd) (**B**) mice are shown. WGA preparations from the Hp/− (**C**) and the myd/myd (**D**) skeletal muscle were also analyzed by western blot using an antibody against α-DG core protein. Laminin-binding activity in Hp/− (**E**) and myd/myd (**F**) mice were measured using solid-phase binding assays and compared to the littermate controls (Hp/+ and myd/+). Open squares (gray line) in panel E indicate laminin-binding activity in wild-type mice.

Reduction of laminin-binding activity due to hypoglycosylation of α-DG is thought to be the main cause of dystroglycanopathy. Therefore, we hypothesized that the minimal levels of intact α-DG species observed in Hp/− mice are sufficient to maintain linkage to laminin and prevent disease progression. To test this hypothesis, we compared the laminin-binding activity in Hp/− mice with that in Large^{myd} (myd/myd) mice, which represent another dystroglycanopathy model with a muscular dystrophy phenotype (21). H&E analysis confirmed signs of muscular dystrophy (centrally located nuclei and fiber size variation) in myd/myd mice, but not in Hp/− mice (Fig. 4A and B). In contrast with Hp/− mice, western blot analysis of α-DG core protein in myd/myd mice revealed no intact size (~150 kDa) of α-DG species (Fig. 4C and D), indicating that almost all α-DG is hypoglycosylated in myd/myd mice. The laminin-binding activity of α-DG in Hp/− and myd/myd mice was measured using a quantitative solid-phase laminin-binding assay and compared with litter controls (Hp/+ and myd/+ mice, respectively) (Fig. 4E and F). Laminin-binding activity was ~50% of normal in Hp/− mice but less than 5% of normal in myd/myd mice. The solid-phase binding analysis shows no obvious difference between wild-type and Hp/+. These data demonstrate that levels of glycosylation (indicated by IIH6 immunoreactivity and the presence of ~150 kDa α-DG) influence laminin-binding activity and indicate that only a small amount of IIH6-reactive α-DG is required to maintain skeletal muscle function.

Fukutin gene transfer restores glycosylation of α-DG in knock-in mice

Our data strongly suggest that even partial restoration of α-DG glycosylation is effective in reducing disease severity in

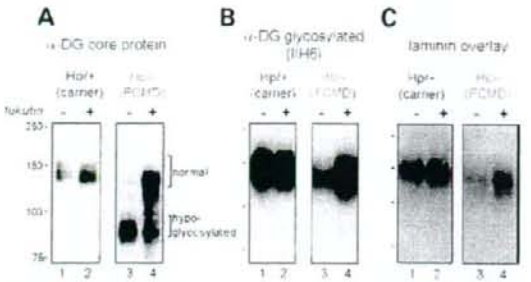

Figure 5. *Fukutin* gene transfer rescues the glycosylation abnormality in Hp/− mice. Hp/+ or Hp/− pups were injected with adenovirus encoding wild-type human *fukutin* in one leg (+) and with saline in the contralateral leg (−). Calf muscle was analyzed using western blot with antibodies against core α-DG protein (**A**) and glycosylated α-DG (**B**) and using a laminin overlay assay (**C**). Transfer of *fukutin* produced increases in α-DG molecular weight, IIH6 reactivity and laminin binding activity in Hp/− mice.

dystroglycanopathy. To examine whether glycosylation defects can be recovered *in vivo*, a recombinant fukutin adenovirus was injected into the hind limb muscle of 3-day-old Hp/− and litter control Hp/+ mice. Following 4 weeks of injections, α-DG enriched samples were prepared using WGA beads and analyzed for glycosylation and laminin-binding activity. Western blot analysis with anti-α-DG core protein antibodies revealed that *fukutin* gene transfer into Hp/− mice reduced hypoglycosylated α-DG (~90 kDa) and increased levels of the normal-sized α-DG species (~150 kDa) (Fig. 5A, lanes 3 and 4). IIH6 reactivity and laminin-binding activity also increased following *fukutin* gene transfer into Hp/− mice (Fig. 5B and C, lanes 3 and 4). No obvious changes were observed in Hp/+ mice after the gene transfer (Fig. 5C, lanes 1 and 2). These results demonstrate that *fukutin* gene transfer can correct biochemical abnormalities of α-DG in *fukutin*-deficient skeletal muscle, and support that fukutin protein is involved in glycosylation of α-DG.

Large gene transfer produces laminin-binding forms of α-DG in dystroglycanopathy models

Hypoglycosylation leading to dystroglycanopathies is caused by mutations in six known genes (*fukutin*, *POMGnT1*, *POMT1*, *POMT2*, *FKRP* and *LARGE*) and other, unidentified genes. In an effort to bypass the need for identification of disease-causing genes in developing therapies (e.g. gene transfer), we further explored a unique feature of LARGE. LARGE has been demonstrated to induce α-DG hyperglycosylation, which is detected by IIH6 as a broad band detected at 150–300 kDa via SDS gel electrophoresis. This band shows increased ligand-binding activity in samples from genetically distinct diseases showing defective α-DG glycosylation (FCMD, MEB and WWS) (26).

We examined whether adenoviral *LARGE* gene transfer into Hp/− skeletal muscle induces hyperglycosylation and increases laminin-binding activity of α-DG. Immunofluorescence analysis of untreated control muscles revealed weaker IIH6 reactivity in Hp/− than in Hp/+ (Fig. 6A, −*LARGE*). Muscle sections subjected to gene transfer showed increased

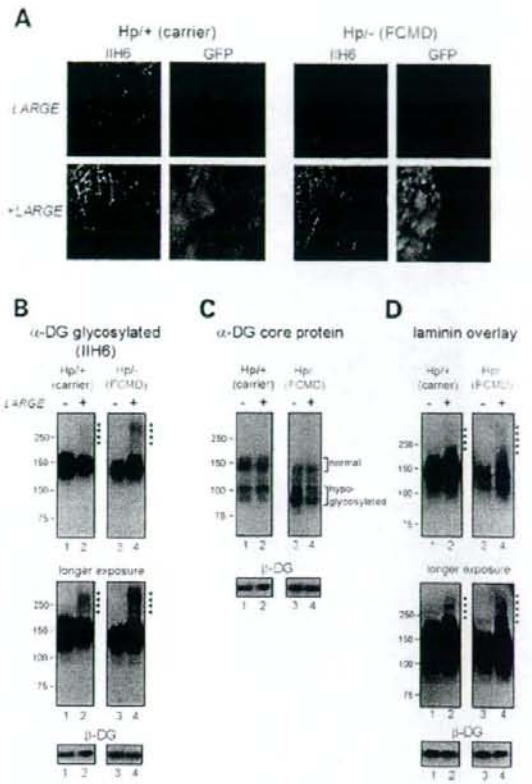

Figure 6. *LARGE* gene transfer produces functionally glycosylated α-DG in Hp/− mice. Hp/+ or Hp/− pups were injected with an adenovirus encoding *LARGE* in one leg (+) and with saline in the contralateral leg (−). Calf muscle was analyzed using IIH6 immunofluorescence (**A**). GFP fluorescence represents muscle fibers successfully transduced by the adenoviral vectors. WGA preparations were analyzed using western blots with antibodies against glycosylated α-DG (**B**), α-DG core protein (**C**) and using a laminin overlay assay (**D**). The western blot for β-DG shows comparable amounts of DG proteins in each lane. Images with longer-exposures better indicate the presence of hyperglycosylated α-DG (arrowheads). These results show that the transfer of *LARGE* increases IIH6 reactivity and laminin-binding activity in Hp/− mice.

α-DG glycosylation in transduced areas, as indicated by eGFP expression in both Hp/− and Hp/+ mice (Fig. 6A, +*LARGE*). We also examined adenovirus-injected and non-injected contralateral leg muscles using western blot analysis with antibodies against α-DG core protein and IIH6. These experiments showed that the *LARGE* gene transfer increased IIH6 reactivity at ~150 kDa in the Hp/− muscle and produced a broad band with a molecular weight of 150–250 kDa in both Hp/− and Hp/+ muscles (Fig. 6B). Anti-α-DG core protein antibodies poorly recognized a higher molecular weight α-DG species (Fig. 6C), which is consistent with previous reports (26). Following the *LARGE* gene transfer, levels of hypoglycosylated α-DG species decreased (Fig. 6C, lanes 3 and 4). These data indicate that

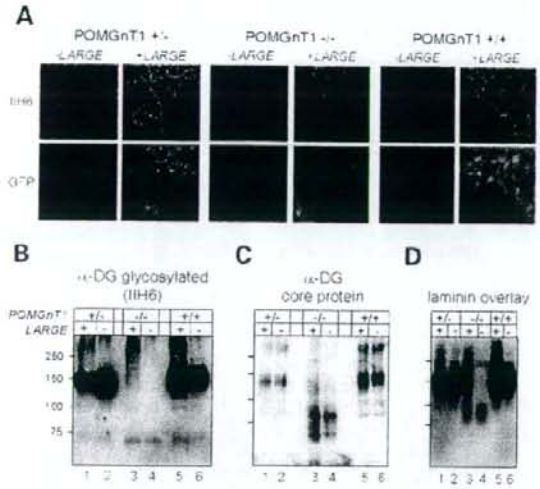

Figure 7. *LARGE* gene transfer produces functionally glycosylated α-DG in MEB disease model mice. POMGnT1$^{+/+}$, POMGnT1$^{+/-}$ or POMGnT1$^{-/-}$ pups were injected with adenovirus encoding *LARGE* in one leg (+*LARGE*) and with saline in the contralateral leg (−*LARGE*). Calf muscle was analyzed using IIH6 immunofluorescence (**A**). GFP fluorescence represents muscle fibers successfully transduced by the adenoviral vectors. WGA preparations were analyzed using western blots with antibodies against glycosylated α-DG (**B**) and α-DG core protein (**C**) and using a laminin overlay assay (**D**). These results show that transfer of *LARGE* increases IIH6 reactivity and laminin-binding activity in POMGnT1$^{-/-}$ mice, the model for MEB disease.

LARGE-induced glycosylation occurs on hypoglycosylated α-DG species. The IIH6-positive broad-molecular-weight band was able to bind laminin in both Hp/− and Hp/+ skeletal muscle samples (Fig. 6D, lanes 2 and 4). These data indicate that LARGE can increase laminin-binding forms of α-DG in *fukutin*-deficient skeletal muscle.

We further investigated whether *LARGE* gene transfer induced hyperglycosylation and produced laminin-binding forms of α-DG species in another dystroglycanopathy model, the *POMGnT1*-disrupted mouse (POMGnT1$^{-/-}$) (Miyagoe-Suzuki *et al.*, manuscript in preparation). Western blot analysis using α-DG core protein antibodies showed a reduction of α-DG molecular weight to 60–90 kDa in POMGnT1$^{-/-}$ mice (Fig. 7C, lane 4). Little IIH6 reactivity was detected via immunofluorescence (Fig. 7A) and western blot (Fig. 7B, lane 4) analysis. These data indicate hypoglycosylation of α-DG in POMGnT1$^{-/-}$ mice. Accordingly, laminin-binding activity was significantly reduced in POMGnT1$^{-/-}$ mice compared with POMGnT1$^{+/-}$ or POMGnT1$^{+/+}$ littermates (Fig. 7D, lanes 2, 4 and 6). The minor laminin binding protein (~80-100 kDa, lane 4) detected only in POMGnT1$^{-/-}$ is unidentified; however, similar laminin binding was also observed in POMGnT1-deficient MEB patients (20). A solid-phase binding assay also showed minor levels of laminin-binding activity in POMGnT1$^{-/-}$ (Supplementary Material, Fig. S4). For all genotypes, adenoviral *LARGE* gene transfer increased IIH6 reactivity in transduced areas indicated by eGFP expression (Fig. 7A, +/+, +/−, and −/−). Western blot analysis using IIH6 showed that *LARGE* gene transfer also induced hyperglycosylation of α-DG in all genotypes, as indicated by broad bands with molecular weights from 150 to >250 kDa (Fig. 7B). After the gene transfer, the POMGnT1$^{-/-}$ skeletal muscle showed only hyperglycosylated IIH6-positive species, while the POMGnT1$^{+/+}$ and the POMGnT1$^{+/-}$ muscles showed both hyperglycosylated and the original 150 kDa IIH6-positive species. Overlay assays showed that the laminin-binding epitope was produced on hyperglycosylated α-DG (Fig. 7D). These data support the idea that LARGE is an effective target for increasing or restoring laminin-binding activity of α-DG in dystroglycanopathy.

DISCUSSION

We have used several approaches to generate FCMD model animals. Fukutin-null mice result in embryonic lethality (27). Fukutin-chimera mice derived from ES cells targeted for both *fukutin* alleles (28) develop muscular dystrophy, but are inappropriate therapeutic study models because (i) they show wide variation in disease severity, and (ii) muscle cell fusion events during growth and regeneration can alter the population of fukutin-null cells. Therefore, we decided to introduce the disease-causing retrotransposon into the mouse *fukutin* gene to mimic the most prevalent form of human FCMD. In these knock-in Hp/Hp and Hp/− mice, we detected hypoglycosylated α-DG, as is seen in FCMD patients (20,31), so we consider them to be novel models for FCMD.

Spontaneous Large^{myd} and Large^{vls} mice (21,32) and genetically engineered POMGnT1-deficient mice (33) have been reported as dystroglycanopathy models. Because these models mimic null mutations such as nonsense and frameshift mutations, they do not necessarily represent human diseases caused by missense mutations. Our knock-in mice with the retrotransposal *fukutin* insertion are the first dystroglycanopathy model that carries a human disease-causing mutation. Such models are needed to explain the molecular pathogenesis of diseases, to determine the function of responsible genes and to screen drugs that correct specific defects (34).

Although these mice genetically and biochemically represent features of *fukutin*-deficient muscular dystrophies, histological analysis has revealed no signs of muscular dystrophy. In typical cases of FCMD, normal-sized α-DG with IIH6-reactivity is barely detected, and laminin-binding activity is dramatically reduced (20). Comparing Hp/− mice with Large^{myd} mice led us to reason that the remaining intact α-DG and laminin-binding activity in Hp/− mice might be sufficient to prevent disease progression. In the future, it would be important to elucidate the threshold level of glycosylation required to avoid a phenotype by using a model system that can control glycosylation levels *in vivo*. In Hp/− mice, residual laminin-binding is detected from DG species with slightly lower molecular weight (<150 kDa) (Fig. 2F), whereas this is not the case for human patients even with retained laminin binding (35). The difference suggests that mice may have additional laminin-binding epitopes, which are less susceptible to fukutin defects. Alternatively, other factors may compensate for

reduced laminin-binding to α-DG. For example, it has been suggested that integrin α7, another laminin receptor in skeletal muscle, may account for the difference in clinical severity between mice and humans with dystrophin- or the DGC-defects (36,37). Clarifying the factors involved would be necessary for a better understanding of pathomechanism, which could promote identification of novel therapeutic targets.

Also important is the finding that even a small amount of IIH6-immunoreactivity of α-DG is sufficient to maintain skeletal muscle function. This concept is supported by milder cases of human patients with fukutin mutations (35). Murakami *et al.* have described reduced but detectable IIH6-reactivity and intact α-DG in patients who are compound heterozygous for the *fukutin* retrotransposon insertion and a missense mutation (R179T or Q358P). These individuals showed minimal dystrophic features and normal intelligence. Laminin-binding activity is also retained in all cases. These findings provide further evidence that the disease severity of fukutin-deficient muscular dystrophy is related to the ratio of normal glycosylation to hypoglycosylation.

Such correlation has been observed in other dystroglycanopathies. LGMD2I patients at the severe end of the clinical spectrum tend to show the greatest reduction in α-DG glycosylation, while those at the milder end tend to have relatively well-preserved α-DG glycosylation (38). Most known missense mutations in *POMGnT1* disrupt POMGnT enzyme activity, causing hypoglycosylation of α-DG and a severe congenital muscular dystrophy phenotype (39,40). Clement *et al.* (6) have reported a patient with a milder LGMD phenotype who carries a novel homozygous missense mutation in *POMGnT1*. Studies of this patient's fibroblasts showed an altered kinetic profile but intact enzyme activity, explaining the relatively mild phenotype. Furthermore, a recent systematic and large-scale study of genotype–phenotype correlation in dystroglycanopathy revealed a wide spectrum of clinical severity in specific disease-causing genes (18). A broad correlation between the amount of depleted glycosylated epitope and phenotypic severity was described, though not systematically quantified. A more recent study reported a few cases with less correlation between clinical course and α-DG immunolabeling (41). We propose that, in addition to immunolabeling, combination of western blotting and laminin binding assays will be necessary for further advances in both clinical and basic biomedical research.

The present study strongly suggests that full recovery of α-DG glycosylation is not always necessary; partial restoration of α-DG glycosylation might be enough to prevent or slow disease progression. The simplest way to restore α-DG glycosylation in dystroglycanopathies would be by replacing a defective gene with the normal version. In many cases, though, the disease-causing gene is not known. A recent study revealed that most patients with a dystroglycanopathy harbor mutations in novel genes (18). To increase amounts of glycosylated α-DG with laminin-binding activity regardless of the responsible gene, we took advantage of the observation that overexpression of LARGE can produce hyperglycosylated α-DG with increased laminin-binding activity in cells from genetically distinct dystroglycanopathies (26). LARGE-induced hyperglycosylation of α-DG has also been observed in both CHO glycosylation mutants showing defective transfer of sialic acid, galactose or fucose to glycoconjugates and in a mutant that is unable to synthesize *O*-mannose glycan (42). Such a 'super-effect' of LARGE on α-DG glycosylation has been observed *in vitro*, but no *in vivo* study has been reported except in Large^{myd} mice (26). Gene transfer of *LARGE* into Large^{myd} mice essentially replaces the defective gene with the normal version of the gene. Our results provide the first *in vivo* evidence that *LARGE* gene transfer can bypass the glycosylation defects of α-DG in models other than the Large^{myd} mice. These results support the idea that glycotherapies aimed at modulating LARGE may be a therapeutic option for many α-DG glycosylation-deficient muscular dystrophies.

Overall, our biochemical, histological and gene transfer experiments using novel model mice with disease-causing mutations support the efficacy of glycotherapy in dystroglycanopathies. The models developed here will be powerful in understanding the pathomechanism of FCMD and other related diseases.

MATERIALS AND METHODS

Generation of model mice

A targeting vector containing the retrotransposal insertion of human FCMD patients was generated using a site-directed DNA integration technique (43). Briefly, lox71 and TK-loxP-neo pA fragments (44) were inserted 5′ and 3′ to exon 10 of mouse *fukutin* (Fig. 1A, no. 2). To excise a floxed part of exon 10 (Fig. 1A, no. 3 Δexon10), Cre was expressed in mouse embryonic stem (ES) cells. Meanwhile, lox66 and TK-loxP fragments were inserted 5′ and 3′ to exon 10 of human *fukutin*, with or without a retrotransposal insertion (Fig. 1A, nos 4 and 5). Each construct was co-transfected with a Cre-expressing vector into ES cells that constitutively express the Δexon10 construct, to obtain recombinant knock-in alleles (Fig. 1A, nos 6 and 7). The transgenic alleles containing normal human exon 10 and mutant exon 10 were named Hn (representing 'human normal') and Hp (representing 'human patient'), respectively. Targeted ES cell clones were injected into blastocysts, and germline-competent heterozygous mice were in turn mated to generate homozygous mutants.

Genotyping of each transgene was performed using PCR with the following primers: FCMDKIF1, GAAACTCTGCCATGACACCTC: HNC440R, ACCAGCTTAAATGCCCAGAAG: Wild R2, GAAGCCAACTGTGTACCACAC. The FCMDKIF1 and HNC440R, and FCMDKIF1 and Wild R2 primer pairs yielded bands of ~800 bp (knock-in allele) and ~1100 bp (wild-type allele), respectively. Genotyping of a *fukutin* allele disruption by a neo replacement (*fukutin* null) was described previously (45). The primers for *fukutin* RT–PCR are AGGGAATGGGCTGGTAGACT and GTGCCATT TTGGGACAAGTT.

C57BL/6 mice were obtained from Japan SLC, Inc., and Large^{myd} mice were obtained from The Jackson Laboratory. Mice were maintained in accordance with the animal care guidelines of Otsuka Pharmaceutical Co. Ltd. and Osaka University.

Antibodies

Antibodies used in western blots and immunofluorescence were as follows: mouse monoclonal antibody 8D5 against β-DG (Novacastra); mouse monoclonal antibody IIH6 against α-DG (Upstate); and polyclonal anti-laminin (Sigma). We generated goat polyclonal antibodies against α-DG core protein using GST fusion proteins containing the N- or C-terminal domains of mouse α-DG. Antisera (074G) were affinity-purified using an α-DG-Fc fusion protein expressed in HEK293 cells. The purified antibody was named AP-074G-C.

Dystroglycan preparation and western blotting

DG was enriched from solubilized skeletal muscle as previously described (20,29). Briefly, 100 mg of muscle was solubilized in 1 ml of Tris-buffered saline (TBS) containing 1% Triton X-100 and protease inhibitors (Funakoshi). The solubilized fraction was incubated with 30 μl of WGA–agarose beads (Vector Labs) at 4°C for 16 h. Beads were washed three times in 1 ml TBS containing 0.1% Triton X-100 and protease inhibitors. The beads were then either directly boiled for 5 min in SDS–polyacrylamide gel electrophoresis (PAGE) loading buffer (western blot and laminin overlay) or eluted with 300 μl TBS containing 0.1% Triton X-100, protease inhibitors and 300 mM *N*-acetylglucosamine (solid-phase binding assay). Proteins were separated using 7.5% or 10% SDS–PAGE. Gels were transferred to polyvinylidene fluoride (PVDF) membrane (Millipore, Bedford, MA, USA). Blots were probed with DG antibodies and then developed with horseradish peroxidase (HRP)-enhanced chemiluminescence (Supersignal West Pico, Pierce; or ECL Plus, GE Healthcare).

Immunofluorescence and histological analysis

Cryosections (7 μm) were prepared and analyzed using immunofluorescence or H&E staining. Sections were stained for 2 min in hematoxylin, 1 min in eosin and then dehydrated with ethanol and xylenes. For immunofluorescence staining with IIH6, sections were treated with cold ethanol/acetone (1:1) for 1 min, blocked with 5% goat serum in MOM Mouse Ig Blocking Reagent (Vector Laboratories) at room temperature for 1 h and then incubated with primary antibodies diluted in MOM Diluent (Vector Laboratories) overnight at 4°C. The slides were washed with PBS and incubated with Alexa Fluor 488-conjugated anti-mouse IgM antibody (Molecular Probes) at room temperature for 30 min. For GFP detection, sections were fixed with 4% paraformaldehyde in PBS for 10 min, washed with PBS three times and then mounted. Permount® (Fisher Scientific) and TISSU MOUNT® (Shiraimatsu Kikai) were used for H&E staining and immunofluorescence, respectively. Sections were observed under fluorescence microscopy (Leica DMR, Leica Microsystems). For EBD uptake, mice were exercised on a treadmill (MK-680S, Muromachi Kikai) as described (34).

Laminin-binding assay

Laminin-binding activity was examined as previously reported (20) with slight modifications. Laminin overlay assays were performed on PVDF membranes using mouse Engelbreth–Holm–Swarm (EHS) laminin (Sigma). Briefly, PVDF membranes were blocked in laminin-binding buffer (LBB: 10 mM triethanolamine, 140 mM NaCl, 1 mM $MgCl_2$, 1 mM $CaCl_2$, pH 7.6) containing 5% non-fat dry milk followed by incubation with 7.5 nM laminin at 4°C for 12 h in LBB with 3% BSA. Membranes were washed and incubated with anti-laminin (Sigma) at 4°C for 3 h followed by anti-rabbit IgG–HRP at room temperature for 45 min. Blots were developed by enhanced chemiluminescence (Supersignal West Pico, Pierce).

For the solid-phase binding assay, WGA eluates were diluted 1:50 in TBS and coated on polystyrene ELISA microplates (Costar) for 16 h at 4°C. Plates were washed in LBB and blocked for 2 h in 3% BSA in LBB. Mouse EHS laminin was diluted in LBB and applied for 1 h. Wells were washed with 3% BSA in LBB, incubated for 1 h with 1:10,000 anti-laminin (Sigma) followed by anti-rabbit HRP. Plates were developed with *o*-phenylenediamine dihydrochloride and H_2O_2, then reactions were stopped with 2 N H_2SO_4 and values obtained on a microplate reader. The data were fit to the equation $A=B_{max}x/(K_d+x)$, where K_d is the dissociation constant, A is absorbance and B_{max} is maximal binding.

Adenoviral gene transfer

The complete open reading frame of mouse *fukutin* was cloned into the EcoRI site of the pKSCX-EGFP vector (46). The pKSCX-EGFP vector contains IRES-EGFP so that both the *fukutin* and *GFP* genes are expressed bicistronically under the CAG promoter. This expression cassette was digested with SwaI, and then its blunt-ended fragment was ligated into the adenoviral cosmid vector. The recombinant adenoviral vector encoding *fukutin* was generated using the method of Tashiro *et al.* (46).

Generation of the recombinant adenoviral vector encoding *LARGE* has been previously described (26). Amplified adenoviruses were purified using VIVAPURE ADENOPACK 100 (VIVASCIENCE).

In vivo gene transfer was performed with Hp/− and control littermate Hp/+ pups, age 2–4 d. Adenoviruses were injected percutaneously into the calf and hamstring with 1×10^8–1×10^9 particles in 10 μl of saline solution. Mock injections used saline solution only. Four weeks after injection, experimental and control contralateral leg muscles were subjected to immunofluorescence and biochemical analysis.

SUPPLEMENTARY MATERIAL

Supplementary Material is available at *HMG* online.

ACKNOWLEDGEMENTS

We would like to thank past and present members of the Clinical Genetics laboratory for fruitful discussions and scientific contributions. We also thank Norihiro Miyazawa and Takashi Wadatsu for technical supports and Dr Jennifer Logan for help in editing the manuscript.

Conflict of Interest statement. None declared.

FUNDING

This work was supported by the Ministry of Health, Labor and Welfare of Japan (Research on Psychiatric and Neurological Diseases and Mental Health H20-016, and The Research Grant for Nervous and Mental Disorders 17A-10 to T.T.); Japan Society for the Promotion of Science (a Grant-in-Aid for Young Scientists (B) 19790232 to M.K.); Mizutani Foundation for Glycoscience (to K.K.); and the Ministry of Education, Culture, Sports, Science, and Technology of Japan (the 21st Century COE program 14013037). Funding to pay the Open Access charge was provided by Research on Psychiatric and Neurological Diseases and Mental Health H20-016.

REFERENCES

1. Martin, P.T. and Freeze, H.H. (2003) Glycobiology of neuromuscular disorders. *Glycobiology*, **13**, 67R–75R.
2. Muntoni, F., Brockington, M., Torelli, S. and Brown, S.C. (2004) Defective glycosylation in congenital muscular dystrophies. *Curr. Opin. Neurol.*, **17**, 205–209.
3. Brockington, M., Yuva, Y., Prandini, P., Brown, S.C., Torelli, S., Benson, M.A., Herrmann, R., Anderson, L.V.B., Bashir, R., Burgunder, J.-M. *et al.* (2001) Mutations in the fukutin-related protein gene (FKRP) identify limb girdle muscular dystrophy 2I as a milder allelic variant of congenital muscular dystrophy MDC1C. *Hum. Mol. Genet.*, **10**, 2851–2859.
4. Dincer, P., Balci, B., Yuva, Y., Talim, B., Brockington, M., Dincel, D., Torelli, S., Brown, S., Kale, G., Haliloglu, G. *et al.* (2003) A novel form of recessive limb girdle muscular dystrophy with mental retardation and abnormal expression of alpha-dystroglycan. *Neuromuscul. Disord.*, **13**, 771–778.
5. Godfrey, C., Escolar, D., Brockington, M., Clement, E.M., Mein, R., Jimenez-Mallebrera, C., Torelli, S., Feng, L., Brown, S.C., Sewry, C.A. *et al.* (2006) Fukutin gene mutations in steroid-responsive limb girdle muscular dystrophy. *Ann. Neurol.*, **60**, 603–610.
6. Clement, E.M., Godfrey, C., Tan, J., Brockington, M., Torelli, S., Feng, L., Brown, S.C., Jimenez-Mallebrera, C., Sewry, C.A., Longman, C. *et al.* (2008) Mild POMGnT1 mutations underlie a novel limb-girdle muscular dystrophy variant. *Arch. Neurol.*, **65**, 137–141.
7. Yoshida, A., Kobayashi, K., Manya, H., Taniguchi, K., Kano, H., Mizuno, M., Inazu, T., Mitsuhashi, H., Takahashi, S., Takeuchi, M. *et al.* (2001) Muscular dystrophy and neuronal migration disorder caused by mutations in a glycosyltransferase, POMGnT1. *Dev. Cell*, **1**, 717–724.
8. Manya, H., Chiba, A., Yoshida, A., Wang, X., Chiba, Y., Jigami, Y., Margolis, R.U. and Endo, T. (2004) Demonstration of mammalian protein O-mannosyltransferase activity: coexpression of POMT1 and POMT2 required for enzymatic activity. *Proc. Natl Acad. Sci. USA*, **101**, 500–505.
9. Barresi, R. and Campbell, K.P. (2006) Dystroglycan: from biosynthesis to pathogenesis of human disease. *J. Cell Sci.*, **119**, 199–207.
10. Chiba, A., Matsumura, K., Yamada, H., Inazu, T., Shimizu, T., Kusunoki, S., Kanazawa, I., Kobata, A. and Endo, T. (1997) Structures of sialylated O-linked oligosaccharides of bovine peripheral nerve alpha-dystroglycan. The role of a novel O-mannosyl-type oligosaccharide in the binding of alpha-dystroglycan with laminin. *J. Biol. Chem.*, **272**, 2156–2162.
11. Fukuyama, Y., Osawa, M. and Suzuki, H. (1981) Congenital progressive muscular dystrophy of the Fukuyama type - clinical, genetic and pathological considerations. *Brain Dev.*, **3**, 1–29.
12. Taniguchi, M., Kurahashi, H., Noguchi, S., Fukudome, T., Okinaga, T., Tsukahara, T., Tajima, Y., Ozono, K., Nishino, I., Nonaka, I. and Toda, T. (2006) Aberrant neuromuscular junctions and delayed terminal muscle fiber maturation in alpha-dystroglycanopathies. *Hum. Mol. Genet.*, **15**, 1279–1289.
13. Kobayashi, K., Nakahori, Y., Miyake, M., Matsumura, K., Kondo-Iida, E., Nomura, Y., Segawa, M., Yoshioka, M., Saito, K., Osawa, M. *et al.* (1998) An ancient retrotransposal insertion causes Fukuyama-type congenital muscular dystrophy. *Nature*, **394**, 388–392.
14. Kondo-Iida, E., Kobayashi, K., Watanabe, M., Sasaki, J., Kumagai, T., Koide, H., Saito, K., Osawa, M., Nakamura, Y. and Toda, T. (1999) Novel mutations and genotype–phenotype relationships in 107 families with Fukuyama-type congenital muscular dystrophy (FCMD). *Hum. Mol. Genet.*, **8**, 2303–2309.
15. Kobayashi, K., Sasaki, J., Kondo-Iida, E., Fukuda, Y., Kinoshita, M., Sunada, Y., Nakamura, Y. and Toda, T. (2001) Structural organization, complete genomic sequences and mutational analyses of the Fukuyama-type congenital muscular dystrophy gene, fukutin. *FEBS Lett.*, **489**, 192–196.
16. Silan, F., Yoshioka, M., Kobayashi, K., Simsek, E., Tunc, M., Alper, M., Cam, M., Guven, A., Fukuda, Y., Kinoshita, M. *et al.* (2003) A new mutation of the fukutin gene in a non-Japanese patient. *Ann. Neurol.*, **53**, 392–396.
17. de Bernabé, D.B., van Bokhoven, H., van Beusekom, E., Van den Akker, W., Kant, S., Dobyns, W.B., Cormand, B., Currier, S., Hamel, B., Talim, B. *et al.* (2003) A homozygous nonsense mutation in the fukutin gene causes a Walker–Warburg syndrome phenotype. *J. Med. Genet.*, **40**, 845–848.
18. Godfrey, C., Clement, E., Mein, R., Brockington, M., Smith, J., Talim, B., Straub, V., Robb, S., Quinlivan, R., Feng, L. *et al.* (2007) Refining genotype phenotype correlations in muscular dystrophies with defective glycosylation of dystroglycan. *Brain*, **130**, 2725–2735.
19. Cotarelo, R.P., Valero, M.C., Prados, B., Peña, A., Rodriguez, L., Fano, O., Marco, J.J., Martinez-Frias, M.L. and Cruces, J. (2008) Two new patients bearing mutations in the fukutin gene confirm the relevance of this gene in Walker–Warburg syndrome. *Clin. Genet.*, **73**, 139–145.
20. Michele, D.E., Barresi, R., Kanagawa, M., Saito, F., Cohn, R.D., Satz, J.S., Dollar, J., Nishino, I., Kelley, R.I., Somer, H. *et al.* (2002) Post-translational disruption of dystroglycan-ligand interactions in congenital muscular dystrophies. *Nature*, **418**, 417–422.
21. Holzfeind, P.J., Grewal, P.K., Reitsamer, H.A., Kechvar, J., Lassmann, H., Hoeger, H., Hewitt, J.E. and Bittner, R.E. (2002) Skeletal, cardiac and tongue muscle pathology, defective retinal transmission, and neuronal migration defects in the Large(myd) mouse defines a natural model for glycosylation-deficient muscle–eye–brain disorders. *Hum. Mol. Genet.*, **11**, 2673–2687.
22. Grewal, P.K., Holzfeind, P.J., Bittner, R.E. and Hewitt, J.E. (2001) Mutant glycosyltransferase and altered glycosylation of alpha-dystroglycan in the myodystrophy mouse. *Nat. Genet.*, **28**, 151–154.
23. Peyrard, M., Seroussi, E., Sandberg-Nordqvist, A.C., Xie, Y.G., Han, F.Y., Fransson, I., Collins, J., Dunham, I., Kost-Alimova, M., Imreh, S. and Dumanski, J.P. (1999) The human LARGE gene from 22q12.3-q13.1 is a new, distinct member of the glycosyltransferase gene family. *Proc. Natl Acad. Sci. USA*, **96**, 598–603.
24. Longman, C., Brockington, M., Torelli, S., Jimenez-Mallebrera, C., Kennedy, C., Khalil, N., Feng, L., Saran, R.K., Voit, T., Merlini, L. *et al.* (2003) Mutations in the human LARGE gene cause MDC1D, a novel form of congenital muscular dystrophy with severe mental retardation and abnormal glycosylation of alpha-dystroglycan. *Hum. Mol. Genet.*, **12**, 2853–2861.
25. Kanagawa, M., Saito, F., Kunz, S., Yoshida-Moriguchi, T., Barresi, R., Kobayashi, Y.M., Muschler, J., Dumanski, J.P., Michele, D.E., Oldstone, M.B. and Campbell, K.P. (2004) Molecular recognition by LARGE is essential for expression of functional dystroglycan. *Cell*, **117**, 953–964.
26. Barresi, R., Michele, D.E., Kanagawa, M., Harper, H.A., Dovico, S.A., Satz, J.S., Moore, S.A., Zhang, W., Schachter, H., Dumanski, J.P. *et al.* (2004) LARGE can functionally bypass alpha-dystroglycan glycosylation defects in distinct congenital muscular dystrophies. *Nat. Med.*, **10**, 696–703.
27. Kurahashi, H., Taniguchi, M., Meno, C., Taniguchi, Y., Takeda, S., Horie, M., Otani, H. and Toda, T. (2005) Basement membrane fragility underlies embryonic lethality in fukutin-null mice. *Neurobiol. Dis.*, **19**, 208–217.
28. Takeda, S., Kondo, M., Sasaki, J., Kurahashi, H., Kano, H., Arai, K., Misaki, K., Fukui, T., Kobayashi, K., Tachikawa, M. *et al.* (2003) Fukutin is required for maintenance of muscle integrity, cortical histiogenesis and normal eye development. *Hum. Mol. Genet.*, **12**, 1449–1459.
29. Kanagawa, M., Michele, D.E., Satz, J.S., Barresi, R., Kusano, H., Sasaki, T., Timpl, R., Henry, M.D. and Campbell, K.P. (2005) Disruption of perlecan binding and matrix assembly by post-translational or genetic disruption of dystroglycan function. *FEBS Lett.*, **579**, 4792–4796.
30. Matsuda, R., Nishikawa, A. and Tanaka, H. (1995) Visualization of dystrophic muscle fibers in mdx mouse by vital staining with Evans blue:

evidence of apoptosis in dystrophin-deficient muscle. *J. Biochem.*, **118**, 959–964.
31. Hayashi, Y.K., Ogawa, M., Tagawa, K., Noguchi, S., Ishihara, T., Nonaka, I. and Arahata, K. (2001) Selective deficiency of alpha-dystroglycan in Fukuyama-type congenital muscular dystrophy. *Neurology*, **57**, 115–121.
32. Lee, Y., Kameya, S., Cox, G.A., Hsu, J., Hicks, W., Maddatu, T.P., Smith, R.S., Naggert, J.K., Peachey, N.S. and Nishina, P.M. (2005) Ocular abnormalities in Large(myd) and Large(vls) mice, spontaneous models for muscle, eye, and brain diseases. *Mol. Cell Neurosci.*, **30**, 160–172.
33. Liu, J., Ball, S.L., Yang, Y., Mei, P., Zhang, L., Shi, H., Kaminski, H.J., Lemmon, V.P. and Hu, H. (2006) A genetic model for muscle-eye-brain disease in mice lacking protein O-mannose 1,2-N-acetylglucosaminyltransferase (POMGnT1). *Mech. Dev.*, **123**, 228–240.
34. Kobuke, K., Piccolo, F., Garringer, K.W., Moore, S.A., Sweezer, E., Yang, B. and Campbell, K.P. (2008) A common disease-associated missense mutation in alpha-sarcoglycan fails to cause muscular dystrophy in mice. *Hum. Mol. Genet.*, **17**, 1201–1213.
35. Murakami, T., Hayashi, Y.K., Noguchi, S., Ogawa, M., Nonaka, I., Tanabe, Y., Ogino, M., Takada, F., Eriguchi, M., Kotooka, N. *et al.* (2006) Fukutin gene mutations cause dilated cardiomyopathy with minimal muscle weakness. *Ann. Neurol.*, **60**, 597–602.
36. Guo, C., Willem, M., Werner, A., Raivich, G., Emerson, M., Neyses, L. and Mayer, U. (2006) Absence of alpha 7 integrin in dystrophin-deficient mice causes a myopathy similar to Duchenne muscular dystrophy. *Hum. Mol. Genet.*, **15**, 989–998.
37. Allikian, M.J., Hack, A.A., Mewborn, S., Mayer, U. and McNally, E.M. (2004) Genetic compensation for sarcoglycan loss by integrin alpha7beta1 in muscle. *J. Cell Sci.*, **117**, 3821–3830.
38. Brown, S.C., Torelli, S., Brockington, M., Yuva, Y., Jimenez, C., Feng, L., Anderson, L., Ugo, I., Kroger, S., Bushby, K. *et al.* (2004) Abnormalities in alpha-dystroglycan expression in MDC1C and LGMD2I muscular dystrophies. *Am. J. Pathol.*, **164**, 727–737.
39. Manya, H., Sakai, K., Kobayashi, K., Taniguchi, K., Kawakita, M., Toda, T. and Endo, T. (2003) Loss-of-function of an N-acetylglucosaminyltransferase, POMGnT1, in muscle-eye-brain disease. *Biochem. Biophys. Res. Commun.*, **306**, 93–97.
40. Manya, H., Bouchet, C., Yanagisawa, A., Vuillaumier-Barrot, S., Quijano-Roy, S., Suzuki, Y., Maugenre, S., Richard, P., Inazu, T., Merlini, L. *et al.* (2008) Protein O-mannosyltransferase activities in lymphoblasts from patients with alpha-dystroglycanopathies. *Neuromuscul. Disord.*, **18**, 45–51.
41. Jimenez-Mallebrera, C., Torelli, S., Feng, L., Kim, J., Godfrey, C., Clement, E., Mein, R., Abbs, S., Brown, S.C., Campbell, K.P. *et al.* (2008) Comparative study of alpha-dystroglycan glycosylation in dystroglycanopathies suggests that the hypoglycosylation of alpha-dystroglycan does not consistently correlate with clinical severity. *Brain Pathol.*, (DOI 10.1111/j.1750–3639.2008.00198).
42. Patnaik, S.K. and Stanley, P. (2005) Mouse large can modify complex N- and mucin O-glycans on alpha-dystroglycan to induce laminin binding. *J. Biol. Chem.*, **280**, 20851–20859.
43. Xiong, H., Kobayashi, K., Tachikawa, M., Manya, H., Takeda, S., Chiyonobu, T., Fujikake, N., Wang, F., Nishimoto, A., Morris, G.E. *et al.* (2006) Molecular interaction between fukutin and POMGnT1 in the glycosylation pathway of alpha-dystroglycan. *Biochem. Biophys. Res. Commun.*, **350**, 935–941.
44. Araki, K., Araki, M. and Yamamura, K. (1997) Targeted integration of DNA using mutant lox sites in embryonic stem cells. *Nucleic Acids Res.*, **25**, 868–872.
45. Chiyonobu, T., Sasaki, J., Nagai, Y., Takeda, S., Funakoshi, H., Nakamura, T., Sugimoto, T. and Toda, T. (2005) Effects of fukutin deficiency in the developing mouse brain. *Neuromuscul. Disord.*, **15**, 416–426.
46. Tashiro, F., Niwa, H. and Miyazaki, J. (1999) Constructing adenoviral vectors by using the circular form of the adenoviral genome cloned in a cosmid and the Cre-loxP recombination system. *Hum. Gene. Ther.*, **10**, 1845–1852.

Biochemical and Biophysical Research Communications 378 (2009) 634–639

Contents lists available at ScienceDirect

Biochemical and Biophysical Research Communications

journal homepage: www.elsevier.com/locate/ybbrc

Surface plasmon resonance characterization of specific binding of polyglutamine aggregation inhibitors to the expanded polyglutamine stretch

Yuma Okamoto [a,b,1], Yoshitaka Nagai [b,*,1], Nobuhiro Fujikake [b,1], H. Akiko Popiel [b,1], Tohru Yoshioka [c], Tatsushi Toda [b], Takashi Inui [a,*]

[a] Department of Molecular Biology and Cell Informatics, Graduate School of Life and Environment Sciences, Osaka Prefecture University, Sakai, Osaka 599-8531, Japan
[b] Division of Clinical Genetics, Department of Medical Genetics, Osaka University Graduate School of Medicine, Suita, Osaka 565-0871, Japan
[c] Graduate Institute of Medicine, Kaohsiung Medical University, Kaohsiung, Taiwan

ARTICLE INFO

Article history:
Received 12 November 2008
Available online 4 December 2008

Keywords:
Aggregation
Inhibitor
Neurodegeneration
Peptide
Polyglutamine
Surface plasmon resonance

ABSTRACT

Proteins with an abnormally expanded polyglutamine (polyQ) stretch are prone to change their conformations, leading to their aggregation, and cause inherited neurodegenerative diseases called the polyQ diseases. Although screening for polyQ aggregation inhibitors has been extensively performed, many common false-positive hits have been identified so far. In this study, we employed surface plasmon resonance (SPR) to characterize the binding specificities and affinities of polyQ aggregation inhibitors to the expanded polyQ stretch. SPR successfully detected specific binding of polyQ binding peptide 1 (QBP1) to the expanded polyQ stretch (K_d = 5.7 μM), and non-specific binding of Congo red to polyQ proteins independent of their polyQ-length. Binding affinities of polyQ aggregation inhibitors to the expanded polyQ stretch were correlated with their inhibitory effects on polyQ aggregation. We therefore conclude that SPR is a useful technique for screening for specific polyQ aggregation inhibitors as promising therapeutic candidates for the currently untreatable polyQ diseases.

Abnormal expansions of the polyglutamine (polyQ) stretch above 40 residues within various proteins commonly cause inherited neurodegenerative diseases including Huntington disease and various types of spinocerebellar ataxia, which are collectively called the polyQ diseases [1,2]. Proteins with an expanded polyQ stretch are prone to change their conformations and to assemble into β-sheet-rich amyloid-like fibrillar aggregates, resulting in accumulation as inclusion bodies in affected neurons, and eventually cause neurodegeneration [2–4]. Amyloid aggregates are also commonly observed in the brains of patients with various neurodegenerative diseases, such as Alzheimer disease and prion diseases [3]. Conformational changes and aggregate formation of the expanded polyQ proteins are one of the most ideal therapeutic targets, since they are the earliest events in the pathogenic cascade and hence their inhibition is expected to widely suppress various downstream pathogenic events [4].

From a therapeutic point of view, we previously identified polyQ binding peptide 1 (QBP1) that preferentially binds to the expanded polyQ stretch [5], and showed that QBP1 inhibits the β-sheet conformational transition and aggregate formation of the expanded polyQ protein *in vitro* [5–7]. We further showed that QBP1 suppresses polyQ-induced neurodegeneration *in vivo*, indicating its potential as a therapeutic molecule [8–10]. Other groups have also identified small chemical compounds that inhibit polyQ aggregation, such as Congo red (CR) and PGL-135 [11,12]. However, CR has recently been reported to inhibit not only aggregate formation of amyloidogenic proteins but also enzymatic activity of unrelated proteins through formation of promiscuous colloidal aggregates, and such non-specific inhibitors are called chemical aggregators [13,14]. Therefore, it is indispensable to exclude non-specific inhibitors for developing therapies for the polyQ diseases.

In this study, we employed surface plasmon resonance (SPR) to characterize the binding specificities and affinities of polyQ aggregation inhibitors to the expanded polyQ stretch. We successfully show that SPR quantitatively detects specific binding of QBP1 to the expanded polyQ stretch. We therefore conclude that SPR characterization of polyQ aggregation inhibitors is useful for the screening of specific inhibitors as therapeutic candidates for the currently untreatable polyQ diseases.

Materials and methods

Materials. The following peptides were synthesized by solid-phase methods: QBP1, SNWKWWPGIFD; SCR, WPIWSKGNDWF; QBP1-M8, WKWWPGIF; QBP1-C9, WKWWPGIFD; QBP1-N9, SNWK

* Corresponding authors. Fax: +81 42 346 1745 (Y. Nagai), +81 72 254 9474 (T. Inui).
E-mail addresses: nagai@ncnp.go.jp (Y. Nagai), inuit@bioinfo.osakafu-u.ac.jp (T. Inui).
[1] Present address: Department of Degenerative Neurological Diseases, National Institute of Neuroscience, National Center of Neurology and Psychiatry, 4-1-1 Ogawa-Higashi, Kodaira, Tokyo 187-8502, Japan.

0006-291X/$ - see front matter © 2008 Elsevier Inc. All rights reserved.
doi:10.1016/j.bbrc.2008.11.094